Bandyopadhyay, Kamal Kanti

TORSIONAL VIBRATION OF DISSIMILAR MATERIALS CONTAINING A CYLINDRICAL CRACK

City University of New York PH.D. 1982

TORSIONAL VIBRATION OF DISSIMILAR MATERIALS CONTAINING A CYLINDRICAL CRACK

by

Kamal K. Bandyopadhyay

A dissertation submitted to
the Graduate Faculty in Engineering
in partial fulfillment of the requirements
for the degree of
Doctor of Philosophy
The City University of New York

1981

This manuscript has been read and accepted for the Graduate Faculty in Engineering in Satisfaction of the dissertation requirements for the degree of Doctor of Philosophy.

11-9-1981
date

Mumtaz K. Kassir
Chairman of Examining Committee

11/16/81
date

Paul R Kramer
Executive Officer

Jacques E. Benveniste
Prof. Jacques E. Benveniste

David H Cheng
Prof. David H. Cheng

Mumtaz K. Kassir
Prof. Mumtaz K. Kassir

Charles A. Miller
Prof. Charles A. Miller

Supervisory Committee

The City University of New York

ACKNOWLEDGEMENTS

It is a pleasure to express my sincere gratitude to Professor Mumtaz K. Kassir, my mentor, for his superb guidance, invaluable help and continuous encouragement during the period of this research. I wish to thank all the professors in the Advisory Committee and other professors in the Civil Engineering Department for their advice in pursuance of this study.

I gratefully remember the inspiration and transportation provided by Dr. Richard Lung, a friend both in the college and at work. The assistance provided by Michael Nesbitt, William Small, Dominick Gaglione and Alisa Ellis in computer use is gratefully acknowledged. A special thanks goes to Mrs. Annedorle Sreckovich who typed the final version of the dissertation.

I sincerely acknowledge the partial tuition refund provided by my employer, Gibbs & Hill, Inc.

In conclusion, I am immensely grateful to my wife who has forborne all the sufferings without a word of complaint and has been a continuous source of inspiration to buy the most precious gift of success to her husband in this research endeavor. With my greatest pleasure, I offer the entire glory for this dissertation to my beloved wife, Ratna.

K.K.B.

ABSTRACT

TORSIONAL VIBRATION OF DISSIMILAR MATERIALS
CONTAINING A CRYLINDRICAL CRACK

by

Kamal K. Bandyopadhyay

Advisor: Professor Mumtaz K. Kassir

This dissertation studies the torsional vibration of two cylinders of different elastic materials. The two cylindrical media are assumed to be perfectly bonded along their entire contact surface except for a cylindrical crack of finite length near the boundary surface. The time-dependent torsional load is applied on the free surface of the inner cylinder. Both the steady-state and transient vibrations are considered, and the corresponding axisymmetric wave equations are solved separately. The determination of the stress and displacement fields is reduced to the solution of Fredholm integral equations of the second kind in the physical complex plane for the steady-state vibration, and in the Laplace domain for the transient case. The local dynamic stress fields in the vicinity of the crack tip are determined in elementary closed form, and are observed to have square-root singularity like other crack problems in linear elastic fracture mechanics.

To this end, the singularity parameter, k_3, defined as the dynamic stress-intensity factor for the torsional mode (tearing) and known to control the fracture behavior of structural components undergoing torsional oscillations, is calculated for both cases of vibration by solving the Fredholm equations numerically. The numerical solution involves computer programming with complex arithmetic for the steady-state vibration, and numerical inversion of Laplace transform for the transient condition. The results indicate a dynamic amplification of the stress-intensity factor for both cases. For a harmonic input, k_3 increases with the frequency, reaches a peak comparable to resonance, and then rapidly diminishes. The transient response to a sudden application of torsional loading is characterized by producing a similar sharp peak in k_3 at a time comparable to that required for the shear wave to travel the crack depth, and then its value oscillates about and slowly approaches the static value.

Studied also in some detail is the influence of varying the ratio of moduli of rigidity of the cylinders and the length of the crack on the dynamic factor k_3. Such results are useful in the theory of brittle fracture where crack-like flaws are developed in structures subjected to mechanical vibrations and in load transfer problems involving compound cylinders.

TABLE OF CONTENTS

LIST OF FIGURES

NOMENCLATURE

$A(s)$	An arbitrary function of s
a	Radius of the inner cylinder
$B(s), B^*(s), B^{**}(s)$	Arbitrary function of s
b	Radius of contact surface of impingent load
$C(s)$	An arbitrary function of s
$c_i = \frac{G_i}{\rho_i}$	Shear Wave velocity of medium i (i=1,2)
d	Depth of layer
$F(s)$, F_n	Functions of s defined by equations (2.31e), (5.17)
$f(z)$	A function of z defined by equation (2.16)
$f_c(\alpha_1)$	Fourier cosine transform of f(z)
G_i	Shear modulus of medium i (i=1,2)
G	G_1/G_2
$g(t), \bar{g}(t,p)$	Functions defined by equations (2.44) and (3.20d)
$g^*(z), \bar{g}^*(z,p)$	Functions defined by equations (2.21c) and (3.16b)
$H(t)$	Heaviside unit step function of time t
$H(s), H_o, H_n$	Functions of s,n defined by equations (2.20b), (5.12)
h	Depth of the crack
$I_n(x)$	Modified Bessel function of the first kind of order n
i	An integer denoting sequence, order, etc.
$J_n(n)$	Bessel function of order n
$K(\theta,t)$	Kernel of the Fredholm equation
$K_n(x)$	Modified Bessel function of the second kind of order n

$\kappa(x)$	Elliptic integral of the first kind
k_1, k_2, k_3	Stress-intensity factors for the first, second and third mode, respectively.
$L(\eta,\xi)$, $\bar{L}(\eta,\xi,p)$	Kernels of Fredholm equations defined by equations (5.2b) and (5.10b)
$M(\xi), \bar{M}(\xi,p)$	Functions defined by equations (5.2c) and (5.10c)
$N(s), \bar{N}(s,p), N_n$	Functions defined by equations (2.32), (3.19c), (5.16)
n	An integer denoting sequence, order, etc.
n_i	Wave number of shear wave in medium i (i=1,2)
$p, \bar{p}$	A variable used for the Laplace transform
q	A parameter used for numerical inversion of Laplace transform
r	Radial axis of the cylindrical coordinate system
s	A variable
T	Applied torque
$\bar{T} = \frac{c_1 t}{h}$	A dimensionless time variable
t	An arbitrary or time variable
u_r, u_θ, u_z, $\bar{u}_r, \bar{u}_\theta, \bar{u}_z$	Displacement components
$W(z)$	Function defined by equation (2.31d)
x	A variable
y	A parameter used for numerical inversion of Laplace transform
z	A coordinate axis coinciding with the center line of the cylinders

α_i	Function given by $\sqrt{s^2 \pm n_i^2}$
γ_i	Function given by $h\alpha_i$
δ	Small distance
η	A variable
θ	Dimensionless variable = $h\eta$. Also a coordinate axis
λ, λ_{ni}	Dimensionless variables
ξ	A variable
ρ_i	Mass density of medium i
$\phi(t)$, $\phi^*(t)$, $\Phi(t)$ $\bar{\Phi}(t,p)$, $\bar{\Phi}(t,p)$	Auxiliary functions
$\psi(1,p)$	A function given by $\frac{\bar{\Phi}(1,\bar{p})}{\bar{p}}$
ω_i	Angular frequency of shear wave in medium i

Chapter 1

INTRODUCTION

Structural members are often loaded in ways that produce three dimensional stress states. In general, although the loading may appear outwardly simple, a complex state of stress can exist inside the medium, particularly in the neighborhood of mechanical defects or cracks, where the stresses undergo sharp elevation. The effects of stress of this kind can frequently lead to unexpected failure. The purpose of fracture mechanics is to take the dimensions of the initial defects of the material into account and to determine the critical load or displacement applied remotely from the defect that will cause catastrophic failure of the whole structure. Therefore, it is essential to relate the resistance of a structural component to crack propagation to a parameter that can characterize the fracture toughness of the material. The most widely used parameter for assessing the onset of rapid fracture in materials without substantial permanent deformation is the one contained in the theories of Griffith [1][1] and Irwin [2]. This parameter is popularly known as stress-intensity factor. The critical value of the stress-intensity factor (a material property) is the fracture toughness. Once this value is known, the designer

---

[1]Numbers in square brackets indicate references listed on pages 87-89.

can proceed to compute the maximum allowable load a structural component can tolerate for a fixed crack size or the maximum size of flaw that is permitted to exist in the material at a given stress level.

In recent years a variety of crack problems have been solved (a comprehensive summary can be found in the works of Sneddon and Lowengrub [3] and Kassir and Sih [4]) on the assumption that the crack is sufficiently away from the neighboring boundaries, and hence that the redistribution of stresses in a solid is attributed either to the crack geometry or to the mechanical loads applied over a localized portion of a solid. For general loading, the amplitude of the stress field near a crack front can be described by three parameters, k_1, k_2 and k_3, respectively known as the stress intensity factors for the opening mode, edge-sliding mode and the twisting or tearing mode.

The analysis of crack problems becomes more involved when the structure is made by bonding together two or more materials with different mechanical properties. The dissimilar material system is required to act as a single unit in that the loads are transmitted from one material to the next through the interface. The presence of flaws or cracks in one of the materials or at the interfaces could cause high elevation of local stresses and lead to failure if the crack reaches a critical size. Hence, it is important to know the stress state associated with these cracks in the dissimilar material

system. It should be noted that for stress distributions characterized by k_1 and k_2, the analytical stress solution exhibits a peculiar behavior near the tip of an interface crack where the stresses undergo a rapid reversal of sign. This behavior was first discovered in the study of two-dimensional crack problems by Williams [5] and Sih and Rice [6]. When the cracked structural component is subjected to dynamic loading additional difficulties are encountered in their analysis.

In general the literature on elastodynamic problems of cracks is somewhat meager. The main reason for this scarcity is the severe mathematical complexity encountered in finding effective solutions for the crack geometry not covered by the classical method of separation of variables. Of importance in fracture mechanics is the detailed character of the dynamic stresses in the vicinity of the crack point. The far field behavior of the stresses can usually be estimated by means of known techniques with comparative ease.

The dynamics of a crack of fixed length travelling at a constant velocity in a stressed medium of infinite extent have been discussed by Yoffe [7]. Using a criterion of maximum circumferential stress ahead of the crack, she concluded that the crack tends to branch for velocities greater than approximately 0.6 times that of the shear wave velocity. A similar problem was solved later by Craggs [8], who assumes the configuration of a semi-infinite crack extended by tractions

applied near a segment of the crack surfaces. Bilby and Bullough [9] obtained the local distribution of longitudinal shear (or anti-plane shear) stress around the tip of a moving crack. Their work was extended to other crack configuration by McClintock and Sukhatme [10].

A more realistic model of the moving crack problem has been proposed by Brobert [11]. He assumes that the crack tips move in opposite direction with constant velocities and found that the speed of propagation of such a crack cannot exceed the Rayleigh surface wave-velocity. Other related problems are found in the works of Barenblatt et al. [12], Craggs [13] and Kostrov [14].

Another class of dynamic problems of interest is concerned with the effect of time-dependent loading on a stationary crack. If the applied loads fluctuate periodically in time, the resulting stresses and displacements are propagated through the structure in the form of waves. At an obstacle, such as a line crack, these waves are reflected and refracted causing high level local stress intensification about the tips of the crack. The intensity of local stresses depends on the amplitude and/or frequency of the traveling waves. In fact, the problem of the diffraction of polarized harmonic shear waves by a semi-infinite crack is mathematically analogous to the corresponding problem in electromagnetic theory.

Loeber and Sih [15] have developed a method for finding the local stresses produced by the interaction of a finite

crack with stress waves. The scattering phenomenon of plane waves due to the presence of a crack has been discussed qualitatively by other authors.

Transient problems in which a semi-infinite crack appears instantaneously in uniformly stressed medium have been explored by Maue [16] using conical coordinates and by Ang [17] employing the technique of Wiener-Hoph. Baker [18] extended their problem to the case where the crack propagates at a constant velocity after it has appeared suddenly in the stretched elastic body.

To obtain a meaningful limit of the transient crack problem as time increases, Ravera and Sih [19] adopted the model of a finite crack. The surface tractions were prescribed as an arbitrary function of time. Their method is particularly effective in finding dynamic stresses near the singular crack point. From the physical standpoint, it is more clear to discuss the steady-state and transient problem of cracks separately.

So far, the dynamic crack problem investigated by Loeber and Sih [15 and 20], Robertson [21], Embley and Sih [22] are the penny-shaped crack in a homogeneous medium subjected to normal compression and radial shear waves and torsional waves.

The problem to be discussed in this dissertation is the effect of torsional vibration on a finite cylindrical crack lying at the interface of two concentric half-space

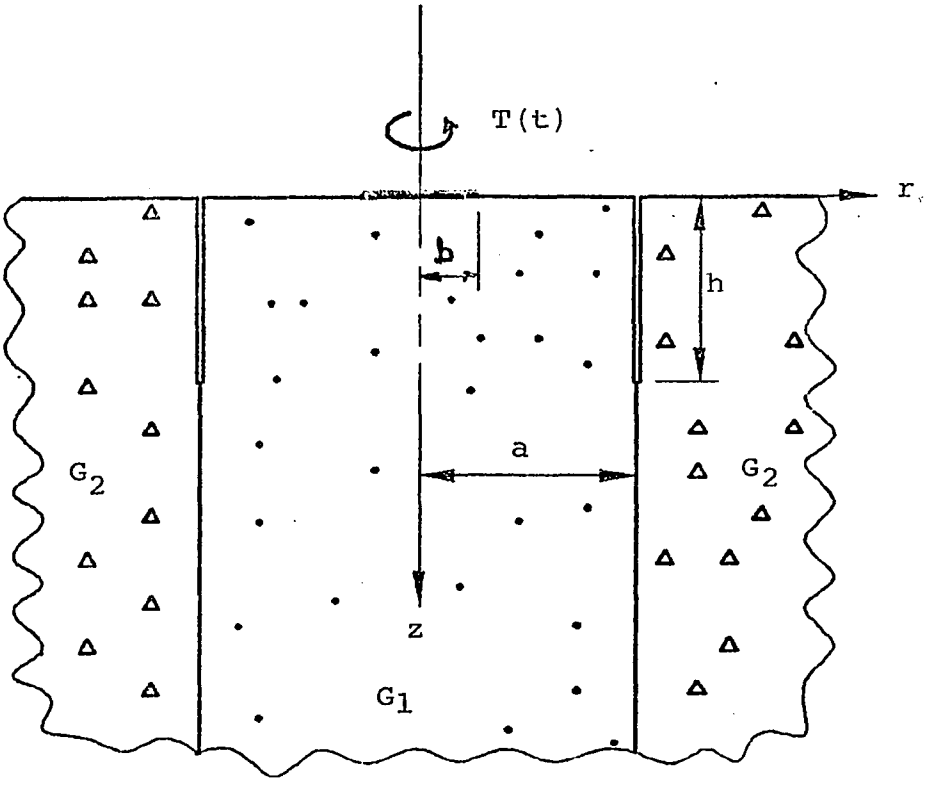

Figure 1. Two concentric cylinders containing a cylindrical crack subjected to dynamic torsion - Half-space

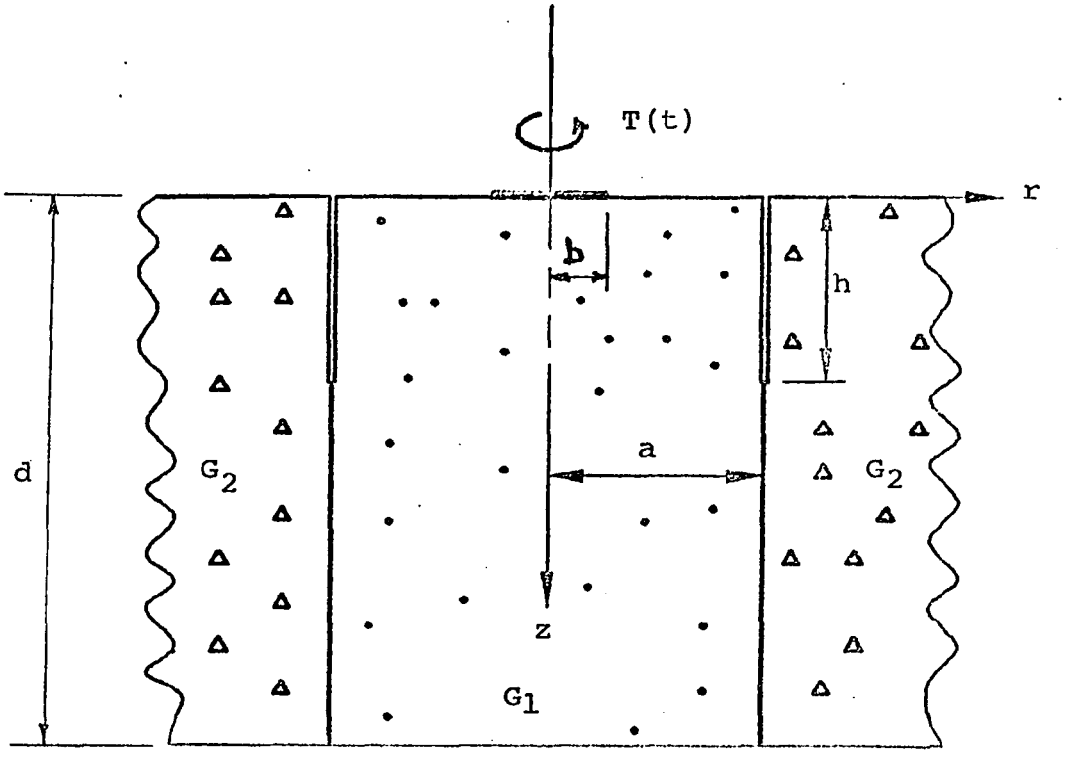

Figure 2. Two concentric cylinders containing a cylindrical crack subjected to dynamic torsion - Layer

cylinders each having different physical properties (Fig. 1). Both the steady state and transient parts of the torsional vibration will be considered separately, and the solution under the static loading will be obtained as a special case. In general, the stress-displacement field will be reduced to quadrature and, in particular, the dynamic stress-intensity factor will be explicitly determined under both steady-state and transient vibrations. Numerical solutions of the dynamic stress-intensity factors will be obtained for different material properties and crack geometry as functions of the shear wave number.

The crack geometry is shown in Fig. 1. The inner cylinder of radius a has a shear modulus G_1. The outer cylinder of a large diameter consists of a different material with the shear modulus G_2. A cylindrical coordinate system (r,θ,z) is used with z-axis coinciding with the longitudinal axis of the two cylinders. The plane $z = 0$ defines the top surface. The crack at the interface extends from the top surface to a depth h, i.e. the crack is defined by cylinder $r = a$, $0 \leq \theta \leq \pi$, $0 \leq z \leq h$. The torsional vibration is generated by known shearing stresses distributed over a circular region of the $z=0$ plane $(0 \leq r \leq b, b < a)$.

In Chapter 2, an integral solution of the fundamental equations of elasticity pertaining to the half-space geometry (Fig. 1), is derived for a steady-state torsional vibration. After imposing the boundary conditions and the regulatory

requirements, the displacement and stress components are expressed in terms of integrals containing Bessel functions of the first kind and modified Bessel functions of the first and second kinds, and an auxiliary function. The auxiliary function is shown to be the solution of a Fredholm equation of the second kind. The dynamic stress-intensity factor for the torsional mode is derived and found to be directly proportional to the solution of the auxiliary function at the crack periphery. The analytical formulation is illustrated by considering two specific steady-state torsional loadings. The first one is concerned with the application of a concentrated torque at a point of the plane boundary, and the second one deals with a torsional stress which varies linearly along the radius of the contact surface. For both examples, the Fredholm integral equations and the expression for stress-intensity factor are simplified and explicitly expressed for numerical treatment.

Chapter 3 deals with the same crack geometry for a transient torsional vibration that may be caused by the application of an impulse twist. The stress and displacement components are transformed to the Laplace domain to eliminate the time variable. Adopting an identical procedure as used in Chapter 2, the dynamic stress-intensity factor is determined in terms of the Laplace inversion of an auxiliary function evaluated at the crack tip. The auxiliary function is the solution of a Fredholm equation in the Laplace plane, which, again, is amenable to numerical treatment. The dynamic

stress-intensity factor follows upon inversion of the Laplace transform solution of the Fredholm equation. For purpose of illustration, the same two spatial variations of the impingent stress distribution as used in the previous chapter are employed here and the corresponding results for the physical quantities of interest are derived.

Chapter 4 studies the behavior of the subject crack under the application of a static torsional load. The solution is obtained as a special case of either the steady-state vibration or the transient vibration discussed in Chapters 2 and 3, respectively.

In Chapter 5, the steady-state solution outlined in Chapter 2 is modified for application to a layer (Fig. 2) in lieu of a half-space.

The numerical solution of the formulae derived in Chapters 2, 3 and 4 is discussed in detail in Chapter 6. Several difficulties encountered in the numerical treatment are noted, and possible remedies are discussed. Some of these are routine in nature for this kind of problem, and others are pertinent to the cylindrical crack problem under study. For a certain range of the variables in the steady-state vibration, some terms are found to be complex in nature requiring the computer programming for numerical solution to involve complex variables with its subsequent processing for matrix manipulation. On the other hand, for the transient condition, the numerical solution of the Fredholm equation is obtained in the Laplace transform plane with the necessary subsequent numerical inversion to compute the dynamic stress-intensity factor.

To illustrate the results, numerical solutions are obtained for a concentrated dynamic torsional load. The results for both steady-state and transient vibrations are exhibited for various material properties, crack geometrics and shear wave velocities. For both conditions, a significant dynamic overshoot of the stress-intensity factor is observed over the corresponding static value. Since the stress-intensity factor is equivalent to the crack extension force, the dynamic amplification is of particular interest in linear elastic fracture mechanics.

The steady state vibration analysis indicates that the dynamic stress-intensity factor initially increases with the frequency of the impingent torsional wave, reaches a peak, and then diminishes first slowly and then rapidly. The dynamic interaction accounts for a maximum increase of about 80%-100% in the amplitude of the local stress field above that obtained on the basis of the static theory of elasticity. The peak occurs at a wavelength of approximately equal to or less than the crack depth depending upon the material properties. For example, a modulus-ratio of $G_1/G_2 = 3$ induces the peak at about 90% of the wavelength.

For transient vibration, the dynamic stress-intensity factor is observed to increase with the time immediately after the application of the impulse torque reaching a peak soon and then oscillating with decreasing amplitude about the static value. For the particular example considered in this dissertation (G_1/G_2=3,10; a/h=1) the maximum dynamic response is

about 40% greater than the corresponding static value. The first and the only prominent peak occurs at a time two to four times longer, depending on material properties, than the time required for the shear wave in the medium to travel a distance equal to the crack depth, after the first application of the transient load. This dynamic behavior is in general agreement with previous research works with transient torsional load.

Such knowledge of the behavior of the parameter k_3 is essential for a clear understanding of the propagation of cracks in structural components undergoing torsional oscillations, since the value of k_3 is known to control the necessary condition for the onset of crack propagation.

Finally, in Chapter 7 some suggestions are made for future research work employing and extending the technique presented in this dissertation.

Chapter 2

STEADY-STATE METHOD OF SOLUTION

The steady-state torsional vibration of two concentric isotropic elastic cylinders having a finite cylindrical crack at their interface is considered in this chapter (Fig. 1). The inner cylinder is surrounded by a different material of a large diameter such that the system may be modeled by a half-space. The steady-state torsional load is assumed to be applied over a small circular area at the free surface of the inner cylinder.

A general integral transform formulation of the stress-displacement field is presented which reduces the problem to the solution of a set of dual integral equations. The solution of the dual integral equations lead to a Fredholm integral equation of the second kind. A special emphasis is given on study of the stress singularity near the crack tip. The amplitude of the local field, commonly known as the mode III stress-intensity factor, k_3, is obtained for an arbitrary shearing load. This factor is known to influence the propagation of cracks in structural members. To illustrate the results obtained, two torque functions are considered--one producing a constant shear stress and the other resulting in a shear stress which varies linearly along the radius--and the formulas for the corresponding stress-intensity factors are obtained.

The influence of the frequency of vibration on the stress-intensity factor is of primary importance, and is investigated in Chapter 6 with a view towards its use in determining the reliability of structural members. The elastic behavior of the media under a static torsional load for the same crack geometry can easily be obtained as a corrolary, and this is discussed in Chapter 4 in some detail.

The method of solution presented in this Chapter will be modified in Chapter 5 for application to the torsional vibration of a layer.

Basic Equations and Formulations

The geometry of the problem shown in Fig. 1 describes a cylindrical crack of depth h at the interface of two concentric cylinders, the inner one being of radius a. In terms of cylindrical polar co-ordinates r, θ and z, the crack occupies the region

$$r = a, \quad 0 \leq \theta \leq 2\pi, \quad 0 \leq z \leq h$$

The vibration is generated by known shear stresses acting on a circular region

$$0 \leq r \leq b, \quad b < a$$

of the boundary plane $z = 0$ of the inner solid. Since for a steady-state vibration the incident torsional wave varies harmonically in time, the space and time variables in the resulting shear stress may be separated as

$$\tau_{z\theta}(r,t) = \mathrm{Re}[\tau_0(r)e^{i\omega t}] = \tau_0(r)\cos \omega t \qquad (2.1)$$

where $\tau_0(r)$ is the specified stress amplitude and ω is the given circular frequency of vibration.

Because of the axisymmetric nature of a torsional problem, the displacement components in the radial and axial directions vanish everywhere, and the circumferential component does not depend on the angle θ, i.e.

$$u_r = u_z = 0, \quad u_\theta = u_\theta(r,z,t) \tag{2.2}$$

and it can be easily shown that only two of the stress components, $\tau_{r\theta}$ and $\tau_{\theta z}$ are different from zero.

$$\tau_{r\theta} = G\left(\frac{\partial u_\theta}{\partial r} - \frac{u_\theta}{r}\right) \tag{2.3a}$$

$$\tau_{\theta z} = G\frac{\partial u_\theta}{\partial z} \tag{2.3b}$$

Two of the equations of motions are identically satisfied and the remaining one gives

$$\frac{\partial^2 u_\theta}{\partial r^2} + \frac{1}{r}\frac{\partial u_\theta}{\partial^2 r} - \frac{u_\theta}{r^2} + \frac{\partial^2 u_\theta}{\partial z^2} = \frac{1}{c_i^2}\frac{\partial^2 u_\theta}{\partial t^2}, \quad (i=1,2) \tag{2.4}$$

where $c_i = (G_i/\rho_i)^{\frac{1}{2}}$ is the shear wave velocity in medium i with G_i and ρ_i being, respectively, the shear modulus and the mass density of the material.

Since the problem has a steady-state time dependence, the displacement and stresses may be considered to vary harmonically in time, as

$$u_\theta(r,z,t) = \mathrm{Re}[u_\theta^*(r,z)e^{i\omega t}] = u_\theta^*(r,z)\cos\,\omega t \tag{2.5}$$

and

$$\tau_{r\theta}(r,z,t) = \mathrm{Re}[\tau_{r\theta}^*(r,z)e^{i\omega t}] = \tau_{r\theta}^*(r,z)\cos\,\omega t \tag{2.6a}$$

$$\tau_{\theta z}(r,z,t) = \mathrm{Re}[\tau^*_{\theta z}(r,z)e^{i\omega t}] = \tau^*_{\theta z}(r,z)\cos\omega t \quad (2.6b)$$

Substituting equation (2.5) into equation (2.4) and rearranging the terms, a differential equation for u^*_θ is obtained

$$\frac{\partial^2 u^*_\theta}{\partial r^2} + \frac{1}{r}\frac{\partial u^*_\theta}{\partial r} - \frac{u^*}{r^2} + \frac{\partial^2 u^*_\theta}{\partial z^2} + n_i^2 u^*_\theta = 0 \quad (2.7)$$

in which n_i is the wave number defined as

$$n_i^2 = \omega^2/c_i^2 = \omega^2\rho_i/G_i \quad , \ (i=1,2)$$

Note that $\omega = 0$ results in the static condition.

By the usual method of separation of variables, the solution of equation (2.7) leading to bounded displacement and stress at remote distances can be shown to assume the form

$$u^*_\theta(r,z) = \int_o^\infty A(s)J_1(rs)e^{-z\sqrt{s^2-n_i^2}}\,ds \quad (2.8a)$$

and the solution which oscillates in z can be shown to be

$$u^*_\theta(r,z) = \int_o^\infty B(s)\begin{bmatrix} I_1(r\sqrt{s^2-n_i^2} \\ K_1(r\sqrt{s^2-n_i^2} \end{bmatrix}\cos(sz)\,ds \quad (2.8b)$$

In equations (2.8), J_n denotes the Bessel function of the first kind of order n, and I_n and K_n are the modified Bessel functions of the first and second kinds, respectively, of order n. A detailed derivation of equation (2.8) is presented in Appendix A. In equation (2.8b) $I_1(rs)$ is to be used in the region $0 \leq r < a$ and $K_1(rs)$ in the region $r > a$.

Introduce the notation $\alpha_i = (s^2-n_i^2)^{\frac{1}{2}}$, in which there is a branch-cut for $s < n_i$ as discussed by Noble [34].

Noting the stress-displacement relation of equations (2.3) the following displacements and stresses for the two media are obtained by combining equations (2.6) and (2.8).

In the inner medium ($0 \leq r \leq a, \quad 0 \leq z < \infty$)

$$u^*_{\theta_1}(r,z) = \int_0^\infty A(s) J_1(rs) e^{-\alpha_1 z}\, ds + \int_0^\infty B(s) I_1(r\alpha_1) \cos(sz)\, ds \tag{2.9a}$$

$$\frac{1}{G_1}\tau^*_{r\theta_1}(r,z) = -\int_0^\infty s\, A(s) J_2(rs)\, e^{-\alpha_1 z}\, ds + \int_0^\infty \alpha_1 B(s) I_2(r\alpha_1) \cos(sz)\, ds \tag{2.9b}$$

$$\frac{1}{G_1}\tau^*_{\theta z_1}(r,z) = -\int_0^\infty \alpha_1\, A(s) J_1(rs) e^{-\alpha_1 z}\, ds - \int_0^\infty s\, B(s) I\, (r\alpha_1) \sin(sz)\, ds \tag{2.9c}$$

while in the outer medium ($a \leq r < \infty, \quad 0 \leq z < \infty$)

$$u^*_{\theta_2}(rz) = \int_0^\infty C(s) K_1(r\alpha_2) \cos(sz)\, ds \tag{2.10a}$$

$$\frac{1}{G_2}\tau^*_{r\theta_2}(r,z) = -\int_0^\infty \alpha_2 C(s) K_2(r\alpha_2) \cos(sz)\, ds \tag{2.10b}$$

$$\frac{1}{G_2}\tau^*_{\theta z_2}(r,z) = -\int_0^\infty s\, C(s) K_1(r\alpha_2) \sin(sz)\, ds \tag{2.10c}$$

In equations (2.9) and (2.10), subscripts 1 and 2 are used for the displacements, stresses and material parameters to indicate their values in the inner and the outer media respectively. The complete time-dependent stress-displacement field can be obtained by multiplying above expressions by $\cos(\omega t)$ and for that one must ensure that only outward waves prevail for the half-

space. For the layer such question does not arise because the waves will be reflected at the remote boundary
Also, in the same equations, A, B and C are unknown functions of s, and are subject to determination from the boundary conditions.

Boundary Conditions

On the z = 0 plane, the shear stress in equation (2.1) is specified inside the contact surface and vanishes outside, so that

$$\tau_{\theta z_1}(r,0,t) = \begin{cases} \tau_o(r) \cos \omega t, & 0 \leq r \leq b \\ 0, & r > b \end{cases} \qquad (2.11a)$$

while the conditions on the traction-free crack surface require that

$$\tau_{r\theta_1} = \tau_{r\theta_2} = 0, \qquad r = a,\ 0 \leq z \leq h \qquad (2.11b)$$

The dissimilar material system is assumed to have a complete bond at the interface and to act as a single unit in that the loads are transmitted from one material to the other through the interface. This requires the displacements and the radial shear stresses of the two materials to be continuous along the interface outside the crack region, i.e.

for $r = a,\ z > h$

$$u_{\theta_1} = u_{\theta_2}$$
$$\tau_{r\theta_1} = \tau_{r\theta_2} \qquad (2.11d)$$

In addition, at remote distances away from the point of application of loading, all displacement and stresses must vanish.

Separating the time element and using the displacement

and stress functions u_θ^*, $\tau_{r\theta}^*$ and $\tau_{\theta z}^*$, which vary in space as adopted in equations (2.5) and (2.6), the boundary conditions can be shown to be equivalent to

on $z = 0$ plane,

$$\tau_{\theta z_1}^* = \begin{cases} \tau_o(r), & 0 \leq r \leq b \\ 0, & r > b \end{cases} \tag{2.12a}$$

and on $r = a$ cylindrical surface,

$$\tau_{r\theta_1}^* = \tau_{r\theta_2}^* = 0, \quad 0 \leq z \leq h \tag{2.12b}$$

$$\left.\begin{aligned} u_{\theta_1}^* &= u_{\theta_2}^* \\ \tau_{r\theta_1}^* &= \tau_{r\theta_2}^* \end{aligned}\right\} \quad z > h \tag{2.12c}$$

$$\tag{2.12d}$$

Method of Solution

The solution of the unknown functions A, B and C in the relations of equations (2.9) and (2.10), will now be sought with the help of the boundary conditions described in equations (2.12).

The conditions on the $z = 0$ plane in equation (2.12a) when used in conjunction with equation (2.9c) yields

$$\int_o^\infty \alpha_1 A(s) J_1(rs)\, ds = \begin{cases} -\dfrac{\tau_o(r)}{G_1}, & 0 \leq r \leq b \\ 0, & r > b \end{cases}$$

with the help of the usual Hankel inversion theorem, the unknown function A(s) can be obtained as

$$\alpha_1 A(s) = -\frac{1}{G_1} \int_o^b r\, \tau_o(r) J_1(rs)\, dr$$

Using the identity

$$r^2 J_1(rs) = \frac{1}{s}\frac{d}{dr}\left[r^2 J_2(rs)\right]$$

and performing an integration by parts, it follows that

$$\alpha_1 A(s) = -\frac{1}{G_1}\left\{b\tau_o(b)J_2(bs) - \int_o^b r^2 J_2(rs)\frac{d}{dr}\left[\frac{\tau_o(r)}{r}\right]dr\right\} \tag{2.13}$$

The other two variables B and C will be obtained from the conditions on the r = a cylindrical surface.

The conditions on the crack surface described in equation (2.12b), when inserted in equations (2.9b) and (2.10b) yield the following relations for $0 \leq z \leq h$

$$\int_o^\infty \alpha_1 B(s) I_2(a\alpha_1)\cos(sz)\, ds = \int_o^\infty s\, A(s) J_2(as)\, a^{-\alpha_1 z} \tag{2.14a}$$

$$\int_o^\infty \alpha_2\, C(s) K_2(a\alpha_2)\cos(sz)\, ds = 0 \tag{2.14b}$$

while the conditions along the bond surface in equations (2.12c) and (2.12d) provide the additional relations for $z > h$, namely

$$\int_o^\infty [B(s) I_1(a\alpha_1)\cos(sz) - C(s) K_1(a\alpha_2)\cos(sz)]ds = -\int_o^\infty A(s) J_1(as) e^{-\alpha_1 z}\, ds \tag{2.14c}$$

$$\int_o^\infty [G_1\alpha_1 B(s) I_2(a\alpha_1)\cos(sz) + G_2\alpha_2 C(s) K_2(a\alpha_2)\cos(sz)]ds = G_1\int_o^\infty sA(s) J_2(as) e^{-\alpha_1 z}\, ds \tag{2.14d}$$

It is easy to show that equations (2.14a), (2.14b) and (2.14d) can be algebraically manipulated to lead to the following relations valid for all values of z:

$$\int_0^\infty [G_1\alpha_1 B(s) I_2(a\alpha_1) + G_2\alpha_2 C(s) K_2(a\alpha_2)] \cos(sz)\, ds$$

$$= G_1 \int_0^\infty sA(s) J_2(as) e^{-\alpha_1 z} ds \qquad (2.15)$$

Introducing the abbreviations

$$G = G_1/G_2$$

$$f(z) = \int_0^\infty t\, A(t) J_2(at) e^{-\sqrt{t^2-n_1^2}\cdot z}\, dt \qquad (2.16)$$

equation (2.15) can be rewritten as

$$\int_0^\infty [\alpha_1 B(s) I_2(a\alpha_1) + \frac{1}{G}\alpha_2 C(s) K_2(a\alpha_2)] \cos(sz)\, ds$$

$$= f(z), \quad 0 \leq z \leq \infty \qquad (2.17)$$

provided that $G_2 \neq 0$.

Equation (2.17) may be inverted with the help of the Fourier cosine transform to yield

$$\alpha_1 B(s) I_2(a\alpha_1) + \frac{1}{G}\alpha_2 C(s) K_2(a\alpha_2) = \frac{2}{\pi} fc(s) \qquad (2.18a)$$

where fc(s) is the one-dimensional Fourier cosine transform

of the function f(z) defined by

$$f_c(s) = \int_o^\infty f(z)\cos(sz)\, dz \tag{2.18b}$$

It readily follows from equation (2.18a) that

$$C(s) = \frac{G}{\alpha_2 K_2(a\alpha_2)} \left[\frac{2}{\pi} f_c(s) - \alpha_1 I_2(a\alpha_1) B(s)\right] \tag{2.19}$$

Making use of equation (2.19), the unknown function C(s) can be eliminated from equation (2.14c) and the resulting equation becomes

$$\int_o^\infty \left[B(s)H(s)\cos(sz) - \frac{2G}{\pi\alpha_2}\cos(sz)\frac{K_1(a\alpha_2)}{K_2(a\alpha_2)} f_c(s)\right] ds$$

$$= -\int_o^\infty A(s) J_1(as) e^{-\alpha_1 z}\, ds, \quad z > h \tag{2.20a}$$

Here, H(s) stands for the abbreviation

$$H(s) = I_1(a\alpha_1) + G\frac{\alpha_1 I_2(a\alpha_1) K_1(a\alpha_2)}{K_2(a\alpha_2)} \tag{2.20b}$$

Now, equations (2.14a) and (2.20) can be grouped together to form the following set of dual integral equations for the determination of the function B(s)

$$\int_o^\infty \alpha_1 B(s) I_2(a\alpha_1)\cos(sz)ds = f(z), \quad 0 \leq z \leq h \tag{2.21a}$$

$$\int_o^\infty B(s)H(s)\cos(sz)ds = g^*(z), \quad z > h \tag{2.21b}$$

where g*(z) stands for

$$g^*(z) = -\int_o A(\theta) J_1(a\theta) e^{-z\sqrt{\theta^2-n_1^2}}\, d\theta$$

$$+ \frac{2}{\pi} G \int_o^\infty \frac{1}{\alpha_2} \cdot \frac{K_1(a\alpha_2)}{K_2(a\alpha_2)} f_c(s)\cos(sz)\, ds \qquad (2.21c)$$

For convenience of the subsequent algebraic work, the function $f_c(s)$ can be expressed in terms of the specified input stress function by eliminating the variable A(s). From the definitions of f(z) and $f_c(s)$ in equations (2.17a) and (2.18b), respectively, $f_c(s)$ can be written as

$$f_c(s) = \int_o^\infty \cos(sz) \left[\int_o^\infty tA(t) J_2(at) e^{-z\sqrt{t^2-n_1^2}}\, dt \right] dz$$

Interchanging the order of integration and using the identity

$$\int_o^\infty \cos(sz)\, e^{-z\sqrt{t^2-n_1^2}}\, dz = \frac{\sqrt{t^2-n_1^2}}{t^2+\alpha_1^2}$$

it follows that

$$f_c(s) = \int_o^\infty \frac{t\sqrt{t^2-n_1^2}}{t^2+\alpha_1^2} J_2(at) A(t)\, dt$$

Moreover, the function A(t) can be eliminated with the help of equation (2.13) to yield

$$f_c(s) = -\frac{1}{G_1}\int_o^\infty \frac{tJ_2(at)}{t^2+\alpha_1^2}\left\{b\tau_o(b)J_2(bt) - \int_o^b r^2 J_2(rt)\,\frac{d}{dr}\left[\frac{\tau_o(r)}{r}\right]dr\right\}$$

Making use of the identity [23]

$$\int_o^\infty \frac{tJ_2(at)J_2(rt)}{t^2+s^2}\,dt = \begin{cases} I_2(rs)K_2(as), & 0 < r < a \\ I_2(as)K_2(rs), & r > a \end{cases}$$

The following relation is reached

$$f_c(s) = -\frac{1}{G}K_2(a\alpha_1)\left\{b\tau_o(b)I_2(b\alpha_1) - \int_o^b r^2 I_2(r\alpha_1)\frac{d}{dr}\left[\frac{\tau_o(r)}{r}\right]dr\right\}$$

Performing an integration by parts, and noting the identity

$$\frac{d}{dr}\,[r^2 I_2(rs)] = s^2 r^2 I_1(rs)$$

one can condense $f_c(s)$ further, so that its evaluation depends on the applied shear stress only

$$f_c(s) = -\frac{\alpha_1 K_2(a\alpha_1)}{G_1}\int_o^b r\tau_o(r) I_1(r\alpha_1)\,dr \qquad (2.22)$$

Note that once the spacial distribution of the shear stress due to the applied torque is specified, $f_c(s)$ can be explicitly determined as a function of the variable s from equation (2.22).

The last unknown function C(s) obtained as a result of the solution of differential equations can now be expressed in terms of the other function B(s) by inserting equation (2.22) in equation (2.19)

$$C(s) = -G\,\frac{\alpha_1 K_2(a\alpha_1)}{\alpha_2 K_2(a\alpha_2)}\left[\frac{2}{\pi G_1}\int_o^b r\tau_o(r) I_1(r\alpha_1)\,dr + I_2(a\alpha_1)\,B(s)\right] \qquad (2.23)$$

From the above equation, C(s) can be readily determined once B(s) is obtained by solving the dual integral equations (2.21).

Solution of Dual Integral Equations

Because each one of the set of dual integral equations governing B(s) contains a given weight function, the solution will be sought by expressing B(s) as a summation of two new functions, one of which will be determined by algebraic relations established so far, and the other will lead to a standard pair of dual integral equations with known solution [24]. For this purpose, let us write

$$B(s) = B^*(s) + B^{**}(s) \tag{2.24a}$$

where $B^{**}(s)$ is defined by the relation

$$\int_0^\infty B^{**}(s)\, H(s)\, \cos(sz)\, ds = g^*(z), \quad 0 \leq z < \infty \tag{2.24b}$$

Using the definition of $g^*(z)$ from equation (2.21c), and rearranging terms, it follows:

$$\int_0^\infty \left[B^{**}(s)\, H(s) - \frac{2}{\Pi} \frac{G}{\alpha_2} \frac{K_1(a\alpha_2)}{K_2(a\alpha_2)} f_c(s) \cos(sz) \right] ds$$

$$= -\int_0^\infty A(0)\, J_1(a\theta)\, e^{-Z\sqrt{\theta^2 - n_1^2}}\, d\theta, \quad 0 \leq z < \infty$$

Inverting the last equation by the usual Fourier cosine transform and interchanging the order of integration, the

equation governing B**(s) assumes the form

$$B^{**}(s)\ H(s) - \frac{2}{\pi}\frac{G}{\alpha_2}\frac{K_1(a\alpha_2)}{K_2(a\alpha_2)}\ f_c(s)$$

$$= \frac{2}{\pi}\int_0^\infty \frac{(\theta^2-n_1^2)^{\frac{1}{2}}}{\theta^2+\alpha_1^2}\cdot A(\theta)\ J_1(a\theta)\ d\theta \qquad (2.25)$$

The identity

$$\int_0^\infty \cos(sz)\ \ e^{-z(\theta^2-n_1^2)^{\frac{1}{2}}}dz = \frac{(\theta^2-n_1^2)^{\frac{1}{2}}}{\theta^2+\alpha_1^2} \qquad (2.26)$$

was used to obtain the above relation. In equation (2.25), A(θ) can be eliminated with the help of equation (2.13) to yield

$$B^{**}(s)H(s) - \frac{2}{\pi}\frac{G}{\alpha_2}\frac{K_1(a\alpha_2)}{K_2(a\alpha_2)}f_c(s) = \frac{2}{\pi G_1}\left\{b\ \tau_o(b)\cdot\right.$$

$$\left.\int_0^\infty \frac{J_1(a\theta)\ J_2(b\theta)d\theta}{\theta^2+\alpha_1^2} - \int_0^b r^2\frac{d}{dr}\left[\frac{\tau_o(r)}{r}\right]\cdot\left[\int_0^\infty \frac{J_1(a\theta)J_2(r\theta)}{\theta^2+\alpha_1^2}\ d\theta\right]dr\right\}$$

Making use of the known result [23]

$$\int_0^\infty \frac{J_1(a\theta)\ J_2(r\theta)d\theta}{\theta^2+s^2} = \frac{1}{s}\ I_2(rs)K_1(as), \quad r < a < \infty$$

it follows

$$B^{**}(s)\ H(s) - \frac{2G}{\pi\alpha_2}\ \frac{K_1(a\alpha_2)}{K_2(a\alpha_2)}f_c(s)$$

$$= \frac{2K_1(a\alpha_2)}{\pi\ G_1}\int_0^b r\ I_1(r\alpha_1)\tau_o(r)\ dr$$

Inserting the value of $f_c(s)$ from equation (2.22) in the

above equation, B**(s) can be obtained in terms of the applied stress distribution as

$$B^{**}(s) = \frac{2}{\pi} \frac{K_1(a\alpha_2)}{H(s)} \left\{ \frac{1}{G_1} - \frac{\alpha_1 K_2(a\alpha_1)}{G_2 \alpha_2 K_2(a\alpha_2)} \right\} \int_o^b r I_1(r\alpha_1) \tau_o(r) dr \quad (2.27)$$

One of the two components of the variable B as defined in equation (2.24a) is thus obtained. The remaining unknown component, B*, will now be sought from equation (2.21). Inserting the definition of B(s) from equation (2.24a) in equations (2.21), the dual integral equations can be written as

$$\int_o^\infty \alpha_1 [B^*(s) + B^{**}(s)] \, I_2(a\alpha_1) \cos(sz) ds = f(z), \quad 0 \leq z \leq h \quad (2.28a)$$

$$\int_o^\infty [B^*(s) + B^{**}(s)] \, H(s) \cos(sz) ds = g^*(z), \quad z > h \quad (2.28b)$$

B** has been chosen in equation (2.24b) such that equation (2.28b) readily takes the form

$$\int_o^\infty B^*(s) \, H(s) \cos(sz) \, ds = 0, \quad z > h \quad (2.29)$$

The other integral equation with B* can be obtained from equation (2.28a) by eliminating B**(s) with the help of equation (2.27), and it follows

$$\int_0^\infty \alpha_1 B^*(s)\ I_2(a\alpha_1)\cos(sz)\,ds$$

$$= f(z) - \frac{2}{\pi}\int_0^\infty \alpha_1 I_2(as)\cos(sz)\cdot\frac{K_1(a\alpha_1)}{H(s)}\left(\frac{1}{G_1} - \frac{\alpha_1 K_2(a\alpha_1)}{G_2\alpha_2 K_2(a\alpha_2)}\right)\cdot$$

$$\cdot\left[\int_0^b r\,\tau_0(r)\ I_1(a\alpha_1)dr\right] ds\ ,\quad 0 \leq z \leq h \qquad (2.30)$$

Equations (2.29) and (2.30) can be written more conveniently in the form

$$\int_0^\infty sN(s)\ F(s)\cos(sz)\ ds = (1+G)\ W(z),\quad 0 \leq z \leq h \qquad (2.31a)$$

$$\int_0^\infty N(s)\cos(sz)\ ds = 0,\qquad z > h \qquad (2.31b)$$

in which the following contractions have been adopted

$$N(s) = B^*(s)\ H(s) \qquad (2.31c)$$

$$W(z) = f(z) - \frac{2}{\pi}\int_0^\infty \alpha_1 I_2(a\alpha_1)\cos(sz)\cdot\frac{K_1(a\alpha_2)}{H(s)}\cdot$$

$$\left(\frac{1}{G_1} - \frac{\alpha_1 K_2(a\alpha_1)}{G_2\alpha_2 K_2(a\alpha_2)}\right)\left[\int_0^b r\ I_1(r\alpha_1)\tau_0(r)\ dr\right]ds \qquad (2.31d)$$

$$F(s) = (1+G)\alpha_1 I_2(a\alpha_1)/[sH(s)] \qquad (2.31e)$$

In order to solve the dual integral equations (2.31), an auxiliary function $\phi^*(t)$ is now introduced such that equation (2.31b) is automatically satisfied. This is accomplished by letting

$$N(s) = \int_0^h \phi^*(t)\ J_0(st)\ dt \qquad (2.32)$$

where $J_o(st)$ is the zero-order Bessel function of the first kind. With this substitution, equation (2.31a) leads to the following Fredholm equation of the second kind for the function $\phi^*(t)$

$$\phi^*(t) + \int_o^h \phi^*(\theta) K^*(\theta,t)\, d\theta = \frac{2(1+G)}{\pi} t \int_o^t \frac{W(z)\,dz}{(t^2-z^2)^{\frac{1}{2}}} \qquad (2.33a)$$

in which the kernel stands for

$$K^*(\theta,t) = t \int_o^\infty s[F(s) - 1]\, J_o(st) J_o(s\theta)\, ds \qquad (2.33b)$$

The derivation of the above solution is detailed in Appendix B. Note that the integral on the right hand side of equation (2.33a) can be expressed in terms of the shear loading as follows (see Appendix C for details).

$$\int_o^t \frac{W(z)\,dz}{(t^2-z^2)^{\frac{1}{2}}} = -\int_o^\infty \left[\frac{\alpha_1 K_2(a\alpha_1)}{G_1} + \frac{1}{G_1} - \frac{\alpha_1 K_2(a\alpha_1)}{G_2 \alpha_2 K_2(a\alpha_2)}\right. \qquad (2.34)$$

$$\left. \alpha_1 I_2(a\alpha_1) \frac{K_1(a\alpha_1)}{H(s)}\right] J_o(st) \left[\int_o^b r I_1(r\alpha_1) \tau_o(r)\, dr\right] ds$$

For convenience of subsequent processing, redefine $\phi^*(t)$ as

$$\phi^*(t) = t^{\frac{1}{2}} \phi(t) \qquad (2.35)$$

so that the Fredholm equation can be written as

$$\phi(t) + \int_o^h \phi(\theta) K(\theta,t)\, d\theta = t^{\frac{1}{2}}\, g(t) \qquad (2.36a)$$

where the symmetrical kernel is now

$$K(\theta,t) = (\theta t)^{\frac{1}{2}} \int_0^\infty s[F(s)-1]J_0(st)J_0(s\theta)ds \qquad (2.36b)$$

and g(t) stands for

$$g(t) = -\frac{2(1+G)}{\pi}\int_0^\infty \left[\frac{\alpha_1 K_2(a\alpha_1)}{G_1} + \left\{\frac{1}{G_1} - \frac{\alpha_1 K_2(a\alpha_1)}{G_2\alpha_2 K_2(a\alpha_2)}\right\}\alpha_1 I_2(a\alpha_1)\frac{K_1(a\alpha_1)}{H(s)}\right]$$

$$\cdot J_0(st)\left[\int_0^b rI_1(r\alpha_1)\tau_0(r)dr\right]ds \qquad (2.36c)$$

The auxiliary function $\phi(t)$ can be obtained numerically from equations (2.36), and subsequently other quantities of physical interest, such as stress-intensity factor and crack surface displacements, can be obtained.

Stress-Intensity Factor

The mathematical theory of brittle fracture mechanics is mainly concerned with the determination of the stress field in the neighborhood of a sharp crack where extension of the crack is imminent. The object, therefore, is to extract the singular contribution from the stress field and obtain the coefficient which govern the strength of the singularity. This coefficient is known as stress intensity factor, k_3, and, for torsional loading, is associated with the tearing mode of extension of the crack surface.

To have a quantitative knowledge of the asymptotic behavior of the stresses around the crack border, let r_1 and θ_1 be the set of local polar coordinates measured from the periphery of the crack border as shown in Figure 3.

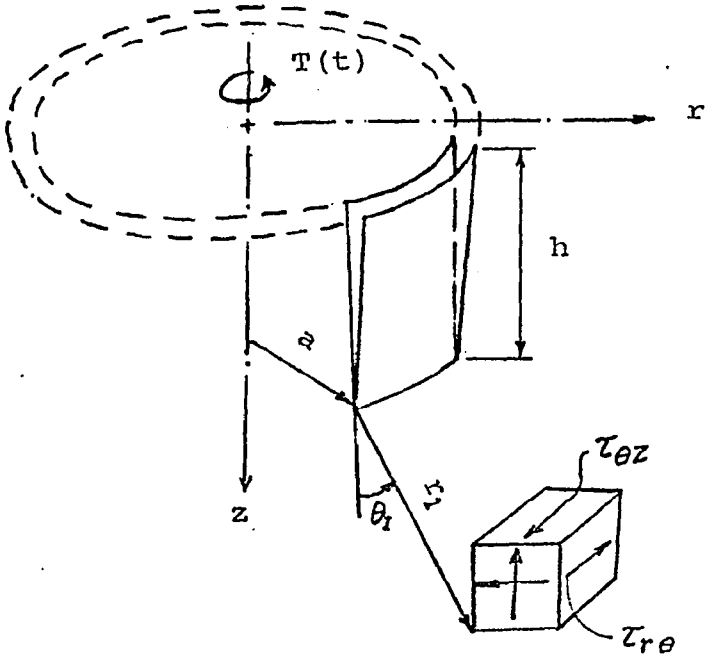

Figure 3. Stress field in the vicinity of crack tip

The local stress state can be expressed in a form which is independent of the crack geometry and loading conditions, and is given by

$$\tau_{r\theta} = \frac{k_3}{(2r_1)^{\frac{1}{2}}} \sin\left(\frac{\theta_1}{2}\right) + O(r_1^{\,0}) \tag{2.37a}$$

$$\tau_{\theta z} = \frac{k_3}{(2r_1)^{\frac{1}{2}}} \cos\left(\frac{\theta_1}{2}\right) + O(r_1^{\,0}) \tag{2.37b}$$

where $\tau_{r\theta}$ and $\tau_{\theta z}$ denote stresses at r_1 and θ_1 away from the crack tip.

In order to derive an explicit expression for k_3, start with equation (2.32) and study the behavior of the function $N(s)$.

Making use of the identity

$$tJ_o(st) = \frac{1}{s} \frac{d}{dt}[tJ_1(st)]$$

and integrating by parts, equations (2.32) with the help of equation (2.35), yield

$$N(s) = \frac{1}{s}\left\{\left[t^{\frac{1}{2}}(t)J_1(st)\right]_{t=0}^{t=h} - \int_o^h t\, J_1(st)\, \frac{d}{dt}\left[\frac{\phi(t)}{t^{\frac{1}{2}}}\right] dt\right\}$$

Noting that the second part of the right side expression does not contribute to the expression for k_3, $N(s)$ can be written as

$$N(s) = \frac{h^{1/2}}{s}\phi(h)\ J_1(hs) + \ldots \tag{2.38}$$

Now, let us examine the shear stress $\tau_{r\theta}$ in the vicinity of the crack tip, i.e. for $r = a$, $z = h+\delta$, where δ is small. For such a location, equation (2.9b) shows with the help of equation (2.13) that the shear stress can be written as

$$\tau^*_{r\theta_1}(a,z) = G_1\int_0^\infty \alpha_1 B(s) I_2(a\alpha_1)\cos(sz)\,ds + \ldots, \quad z > h$$
where the dots indicate non-singular terms. (2.39)

Finally, making use of equations (2.24a), (2.27) and (2.28), and expressing all unknown variables in terms of the specified stress function, $\tau(r)$ and the auxiliary function $\phi(t)$, $\tau^*_{r\theta_1}$ can be rewritten from equation (2.39) as

$$\tau^*_{r\theta_1}(a,z) = \frac{2G_1}{\pi}\int_0^\infty \frac{\alpha_1 K_1(a\alpha_1) I_2(a\alpha_1)}{H(s)}\left(\frac{1}{G_1} - \frac{\alpha_1 K_2(a\alpha_1)}{G_2\alpha_2 K_2(a\alpha_2)}\right)\left[\int_0^b rI_1(r\alpha_1)\cdot \tau_0(r)\,dr\right]\cos(sz)\,ds + G_1 h^{1/2}\phi(h)\int_0^\infty \frac{\alpha_1}{s}\frac{I_2(a\alpha_1)}{H(s)} J_1(hs)\cdot\cos(sz)\,ds + \ldots,\ z > h \tag{2.40}$$

For large values of s, the following asymptotic behavior of the modified Bessel function is observed [25]

$$I_p(a\alpha_i) \sim \frac{e^{as}}{\sqrt{2\pi as}}$$

$$K_p(a\alpha_i) \sim \frac{e^{-as}}{\sqrt{\frac{2as}{\pi}}}$$

Making use of these relations to search for the singularity

in the shear stress expression, equation (2.40) can be written as

$$\tau^{*}_{r\theta_1}(a,z) = \frac{G_1}{(1+G)\pi}\int_o^\infty \frac{1}{e^{as}\sqrt{as}}\left(\frac{1}{G_1} - \frac{1}{G_2}\right)\cdot\left[\int_o^b \frac{e^{rs}}{\sqrt{rs}}\,\tau_o(r)\,dr\right]\cdot$$

$$\cdot \cos(sz)\,ds + \frac{G_1 h^{\frac{1}{2}}}{1+G}\,\phi(h)\int_o^\infty J_1(hs)\cos(sz)\,ds$$

$$+ \ldots\,, \quad z > h$$

Noting that $a > b$, the first term in the above equation is evidently not singular for a definite specified stress function. The only possible singular term in the above equation is the second term which can be expressed as

$$\tau^{*}_{r\theta_1}(a,z) = \frac{G_1}{1+G}\,\frac{\phi(h)}{h^{\frac{1}{2}}}\left[1 - \frac{z}{\sqrt{z^2-h^2}}\right] + \ldots\,, \quad z > h \qquad (2.41)$$

The following identities were used to arrive at the above equation [23]

$$\int_o^\infty \cos(\beta_1 z)\,J_1(h\beta_1)\,d\beta_1 = \frac{1}{h}\left(1 - \frac{z}{\sqrt{z^2-h^2}}\right), \quad z > h$$

Note that equation (2.41) is singular at the tip of the crack where $z = h$.

To obtain an expression for the stress-intensity factor,

replace z by (h+δ) and expand equation (2.41) as follows

$$\left[\tau^{*}_{r\theta_1}\right]_{\substack{r=a \\ z=h+\delta}} = \frac{G_1}{1+G}\,\frac{\phi(h)}{h^{\frac{1}{2}}}\left[1 - \frac{(1+\frac{\delta}{h})\sqrt{h}}{\sqrt{2\delta}\ \sqrt{1+\frac{\delta}{2h}}}\right] + \cdots$$

separating the singular term and making use of equation (2.6a), the time dependent shear stress can be obtained as

$$\left[\tau_{r\theta_1}\right]_{\substack{r=a \\ z=h+\delta}} = -\frac{G_1}{1+G}\,\frac{\phi(h)}{\sqrt{2\delta}}\cos(\omega t) + 0(\delta^{\circ})$$

At this point, we can define a dynamic stress-intensity factor (Sih [26]) which can be related to the rate of energy release per unit crack extension as in the static case. Following this definition, the local stress distribution must be separated into the product of a spatial component with a square-root singularity of δ and a function of load geometry and time. This is consistent with the static theory of linear fracture mechanics where the crack border stress distribution associated with k_3 is obtained by letting $\delta \to 0$.

Therefore, by definition, the dynamic stress-intensity factor for the torsional mode can be expressed as

$$k_3 = -\frac{G_1}{1+G}\,\phi(h) \qquad (2.42)$$

where $\phi(h)$ is the solution of the Fredholm equation (2.36a) and will be determined numerically in Chapter 6.

Examples

In order to illustrate the use of the formulas derived earlier, the applied shear stress is to be specified. Two different stress distributions will be considered in this dissertation, namely a constant shearing stress and a linearly varying one.

Example 1

Consider the case of a constant shear stress over a small circular region of radius b, i.e.

$$\tau_o(r) = \text{constant} = K, \quad 0 \leq r \leq b$$

The applied torque can be obtained from the specified stress as

$$T = \iint_{\text{Area}} r k dA = \frac{2\pi K}{3} b^3$$

or $$K = \frac{3T}{2\pi b^3}$$

By letting $b \to 0$, the deformation can be considered to be caused by a concentrated torque, T, applied at the origin of coordinates. It follows that the second integral of the right side of equation (2.36c) can be evaluated as

$$\int_o^b r\, I_1(r\alpha_1)\tau_o(r)\, dr = \frac{3T}{2\pi b^3}\int_o^b r I_1(r\alpha_1)\, dr$$

$$\equiv \frac{3T}{2\pi b^3}\frac{d}{d\alpha_1}\left[\int_o^b I_o(r\alpha_1)dr\right]$$

Expanding $I_o(r\alpha_1)$ as [25]

$$I_o(r\alpha_1) = 1 + \frac{r^2\alpha_1^2}{4} + \frac{r^4\alpha_1^4}{64} + \ldots.$$

and performing the integration and differentiation, it follows

$$\int_o^b rI_1(r\alpha_1)\tau_o(r)\ dr = \frac{3T}{2\pi}\left[\frac{\alpha_1}{6} + \frac{\alpha_1^3 b^2}{80} + \ldots\right]$$

For a concentrated torque, $b \to 0$ so that the integral becomes

$$\int_o^b rI_1(a\alpha_1)\tau_o(r)\ dr = \frac{T\alpha_1}{4\pi} \tag{2.43}$$

Inserting equation (2.43) in equation (2.36c)

$$g(t) = -\frac{T(1+G)}{2\pi^2 G_1}\int_o^\infty \alpha_1^2\left[K_2(a\alpha_1) + \left\{1 - \frac{G\alpha_1 K_2(a\alpha_1)}{\alpha_2 K_2(a\alpha_2)}\right\}\cdot I_2(a\alpha_1)\ \frac{K_1(a\alpha_1)}{H(s)}\right]J_o(st)\ ds \tag{2.44}$$

Making use of equation (2.44), the Fredholm equation (2.36a) can be numerically solved for various material properties and shear wave velocities. An elaborate description of the numerical solution is presented in Chapter 6.

Example 2

As a second illustration, consider a torque T producing linear variation of shear stress along the radius of the contact circle, i.e.

$$\tau_o(r) = \tau_o\frac{r}{b} \qquad 0 \leq r \leq b, \quad b < a$$

where τ_o denotes the stress at the periphery of the stressed circle.

The total torque can be obtained as

$$T = \iint_{\text{Area}} \tau_o \frac{r^2}{b} \, dA = \frac{\pi b^3}{2} \tau_o$$

so that

$$\tau_o = \frac{2T}{\pi b^3}$$

Making use of these relations, it follows

$$\int_o^b r I_1(r\alpha_1)\tau_o(r) \, dr = \frac{2T}{Kb^4} \int_o^b r^2 I_1(r\alpha_1) dr \qquad (2.45)$$

Using equation (2.45) in equation (2.36a), it follows that

$$g(t) = -\frac{T(1+G)}{\pi b^4 G_1} \int_o^\infty \left[\alpha_1 K_2(a\alpha_1) + \left(1 - \frac{G\alpha_1 K_2(a\alpha_1)}{\alpha_2 K_2(a\alpha_2)} \right) \cdot \alpha_1 I_2(a\alpha_1) \frac{K_1(a\alpha_1)}{H(s)} \right] J_o(st) \left[\int_o^b r^2 I(r\alpha_1) dr \right] ds \qquad (2.46)$$

and the Fredholm equation can be numerically solved to yield the stress-intensity factor for various materials and wave velocities. This will be accomplished in chapter 6.

Chapter 3

TRANSIENT TORSIONAL VIBRATION

Structural components are often subjected to impulsive loads which generate stress waves. At a certain time, the propagation of these waves can cause high stress intensity in a local region around a geometric singularity such as the crack tip. The magnitude of the dynamic stresses can be considerably larger than the statical ones, and may lead to crack extension and failure. Thus it is desirable to obtain certain useful relations between the parameters of the transient stress waves and the crack dimension.

The transient response of a cylindrical crack due to an impulsive torsional load is investigated in this chapter. The same crack geometry at the interface of two different concentric cylindrical media used for the steady-state solution in Chapter 2 is used to study the transient response. A stress analysis of the cracked body due to transient shear waves generated by the application of a time dependent torque is carried out. In order to eliminate the time variable, a Laplace transform is applied and the remaining analysis is performed in the Laplace transform plane. Once in the transformed plane, the formulation is similar to that for a steady-state vibration, and consequently, wherever possible, the mathematical details are omitted in this chapter by referring

to similar relations already established in Chapter 2.

The use of boundary conditions in the stress-displacement relations leads to a pair of dual integral equations which are solved in the form of a Fredholm equation of the second kind. The dynamic stresses near the periphery of the crack are found to have the same angular distribution and inverse square root singularity as in the steady-state case. However, the stress-intensity factor is different in this case.

Two different impingent stress distributions are used for illustration--one with a constant shear stress and another with a linearly varying shear stress. As in the steady-state case, the static solution can easily be recovered from the transient analysis also, and this solution will be presented in Chapter 4.

The dynamic stress intensity factor is formulated in terms of an inversion of the Laplace transform. The physical stress intensity factor and, in particular, its amplification over the static value can be obtained by numerical procedure. For the class of problem under study, the dynamic overshoot is of the order of 40%. This is discussed in detail in Chapter 6.

Basic Equations and Formulations

The structure shown in Fig. 1 experiences an impulsive torque applied on a circular region $0 \leq r \leq b$, $b < a$, of the plane $z = 0$. The impingent stress is time dependent and its distribution is specified as follows

$$\tau_{z\theta}(r,0,t) = \begin{cases} \tau_o(r)\ H(t), & 0 \leq r \leq b \\ 0 & r > b \end{cases} \qquad (3.1)$$

where $\tau_o(r)$ denotes a known spatial distribution of stress and H(t) designates the usual Heaviside unit step function.

From the axisymmetric nature of the problem, the displacement components u_r and u_z vanish throughout the body and the only nonzero component u_θ is independent of θ, i.e.

$$u_r = u_z = 0, \quad u_\theta = u_\theta(r,z,t) \tag{3.2}$$

The governing differential equation of motion takes the form

$$\frac{\partial^2 u_\theta}{\partial r^2} + \frac{1}{r}\frac{\partial u_\theta}{\partial r} - \frac{u_\theta}{r^2} + \frac{\partial^2 u_\theta}{\partial z^2} = \frac{1}{c_i^2}\frac{\partial^2 u_\theta}{\partial t^2} \quad (i = 1,2) \tag{3.3}$$

where c_i is the shear wave velocity in medium i and is defined in Chapter 2. In order to eliminate the time variable, introduce the Laplace transform pair of u_θ usually defined as follows

$$\bar{u}_\theta(r,z;p) = \int_o^\infty u_\theta(r,z,t)\, e^{-pt}\, dt \tag{3.4a}$$

$$u_\theta(r,z,t) = \frac{1}{2\pi i}\int_{Br} \bar{u}_\theta(r,z;p)\, e^{pt}\, dp \tag{3.4b}$$

where the path of integration in equation (3.4b) is the Bromwich path which is a line on the right-hand side and parallel to the imaginary axis of the p-plane.

Since the initial conditions are

$$u_\theta(r,z,0) = 0 \tag{3.5a}$$

$$\left[\frac{\partial u_\theta}{\partial t}\right]_{\text{at } t=0} = 0 \tag{3.5b}$$

the following relations are readily obtained

$$\int_o^\infty e^{-pt} \frac{\partial u_\theta}{\partial t} dt = p\bar{u}_\theta \tag{3.6a}$$

$$\int_o^\infty e^{-pt} \frac{\partial^2 u_\theta}{\partial t} dt = p^2\bar{u}_\theta \tag{3.6b}$$

Applying these relations, the differential equation (3.3) can be transformed in the p-plane, and the result is

$$\frac{\partial^2 \bar{u}_r}{\partial r^2} + \frac{1}{r}\frac{\partial \bar{u}_\theta}{\partial r} + \frac{\partial^2 \bar{u}_\theta}{\partial z^2} - \frac{\bar{u}_\theta}{r^2} = \frac{p^2}{c_i^2}\bar{u}_\theta \tag{3.7}$$

Equation (3.7) can be solved by the method of separation of variables, and the solutions are

$$\bar{u}_\theta(r,z;p) = \frac{1}{p}\int_o^\infty A(s,p)J_1(sr)e^{-z\sqrt{s^2 + p^2/c_i^2}}\,ds \tag{3.8a}$$

which vanishes for large z, and

$$\bar{u}_\theta(r,z;p) = \frac{1}{p}\int_o^\infty B(s,p)\begin{bmatrix} I_1(r\sqrt{s^2+p^2/c_i^2}) \\ K_1(r\sqrt{s^2+p^2/c_i^2}) \end{bmatrix}\cos(sz)\,ds \tag{3.8b}$$

which oscillates in z. The choice of the modified Bessel functions I_1 or K_1 will be based upon the boundary conditions and be governed by the finiteness requirement of the displacement component as $r \to 0$ and $r \to \infty$.

Introducing the notations

$$\alpha_i = (s^2 + p^2/c_i^2)^{\frac{1}{2}}$$

the following stress and displacement components in the transformed plane are obtained for each medium with the help of equations (3.8) and (2.3):

For the inner cylinder ($0 \leq r \leq a$, $0 \leq z < \infty$)

$$\bar{u}_{\theta_1}(r,z;p) = \frac{1}{p}\int_0^\infty A(s,p)J_1(rs)\, e^{-\alpha_1 z}\, ds + \frac{1}{p}\int_0^\infty B(s,p)I_1(r\alpha_1)\cos(sz)\, ds \tag{3.9a}$$

$$\frac{1}{G_1}\bar{\tau}_{r\theta_1}(r,z;p) = -\frac{1}{p}\int_0^\infty sA(s,p)J_2(rs)e^{-\alpha_1 z}ds + \frac{1}{p}\int_0^\infty \alpha_1 B(s,p)I_2(r\alpha_1)\cos(sz)ds \tag{3.9b}$$

$$\frac{1}{G_1}\bar{\tau}_{\theta z_1}(r,z;p) = -\frac{1}{p}\int_0^\infty A(s,p)J_1(rs)e^{-\alpha_1 z}ds - \frac{1}{p}\int_0^\infty sB(s,p)I_1(r\alpha_1)\sin(sz)\, ds \tag{3.9c}$$

while for the outer cylinder ($a \leq r < \infty$, $0 \leq z < \infty$)

$$\bar{u}_{\theta_2} = \frac{1}{p}\int_0^\infty C(s,p)K_1(r\alpha_2)\cos(sz)\, ds \tag{3.10a}$$

$$\frac{1}{G_2}\bar{\tau}_{r\theta_2} = -\frac{1}{p}\int_0^\infty \alpha_2 C(s,p)K_2(r\alpha_2)\cos(sz)\, ds \tag{3.10b}$$

$$\frac{1}{G_2}\bar{\tau}_{\theta z_2} = -\frac{1}{p}\int_0^\infty sC(s,p)K_1(r\alpha_2)\sin(sz)\, dz \tag{3.10c}$$

In equations (3.9) and (3.10), A, B and C are unknown functions to be determined from the boundary conditions, and the subscripts 1 and 2 for the stress-displacement components

and material properties indicate their values in the inner and the outer cylinder respectively.

Boundary Conditions

On the z = 0 surface of the halfspace, the shear stress $\tau_{\theta z}$ is specified by equation (3.1). Taking Laplace transform of $\tau_{\theta z}$ and noting the fact that the Laplace transform of H(t) is given by

$$\int_0^\infty H(t)e^{-tp}\,dt = \frac{1}{p}$$

it follows that the transformed boundary condition for $\tau_{\theta z}$ in the p-plane becomes

$$\bar{\tau}_{\theta z}(r,0,p) = \begin{cases} \dfrac{\tau_o(r)}{p}, & 0 \leq r \leq b, \quad z = 0 \\ 0, & b > r, \quad z = 0 \end{cases} \tag{3.11a}$$

The remaining boundary conditions and regulatory requirements are identical to those used for the steady-state solution in Chapter 2 [see equations (2.11b), (2.11c) and (2.11d)] and yield the following conditions in the transformed plane

$$\bar{\tau}_{r\theta_1} = \bar{\tau}_{r\theta_2} = 0, \quad 0 \leq z \leq h, \quad r = a \tag{3.11b}$$

$$\bar{u}_{\theta_1} = \bar{u}_{\theta_2}, \quad z > h, \quad r = a \tag{3.11c}$$

$$\bar{\tau}_{r\theta_1} = \bar{\tau}_{r\theta_2}, \quad z > h, \quad r = a \tag{3.11d}$$

Method of Solution

The unknown functions A, B and C as appeared in the stress

and displacement equations (3.9) and (3.10), can now be obtained with the help of the boundary conditions defined by equations (3.11) Since the necessary algebraic manipulations are similar to those given in Chapter 2, only the pertinent results will be presented here.

With the aid of the Hankel inversion theorem, the boundary condition on z = 0 plane in equation (3.11a) leads to the determination of the function A. The result is

$$\alpha_1 A(s,p) = -\frac{1}{G_1}\left\{ b\tau_o(b)J_2(bs) - \int_o^b r^2 J_2(rs)\,\frac{d}{dr}\left[\frac{\tau_o(r)}{r}\right] dr \right\} \qquad (3.12)$$

The remaining boundary conditions in equations (3.11) when applied on equations (3.9) and (3.10), yield the following simultaneous equations for the solution of B and C:

For $0 \leq z \leq h$,

$$\int_o^\infty \alpha_1 B(s,p) I_2(a\alpha_1)\cos(sz)\,ds = \int_o^\infty sA(s,p)J_2(as)e^{-\alpha_1 z}\,ds \qquad (3.13a)$$

$$\int_o^\infty \alpha_2 C(s,p) K_2(a\alpha_2)\cos(sz)\,ds = 0 \qquad (3.13b)$$

and for $z > h$,

$$\int_o^\infty [B(s,p)I_1(a\alpha_1) - C(s,p)K_1(a\alpha_2)\cos(sz)\,ds = -\int_o^\infty A(s,p)J_1(as)e^{-\alpha_1 z}\,ds \qquad (3.13c)$$

$$\int_0^\infty [G_1\alpha_1 B(s,p) I_2(a\alpha_1) + G_2\alpha_2 C(s,p) K_2(a\alpha_2)] \cos(sz)\, ds$$
$$= G_1 \int_0^\infty sA(s,p) J_2(as) e^{-\alpha_1 z}\, ds \qquad (3.13d)$$

Following the same procedure as adopted for the steady-state solution [reference equations (2.15) through (2.21)], the unknown functions B and C can be solved from equations (3.13) as follows:

$$C(s,p) = \frac{G}{\alpha_2 K_2(a\alpha_2)} \left[\frac{2}{\pi} f_c(s,p) - \alpha_1 I_2(a\alpha_1) B(s,p) \right] \qquad (3.14)$$

where $B(s,p)$ is given by the dual integral equations

$$\int_0^\infty \alpha_1 B(s,p) I_2(a\alpha_1) \cos(sz)\, ds = f(z,p), \quad 0 \leq z \leq h \qquad (3.15a)$$

$$\int_0^\infty B(s,p) H(s,p) \cos(sz)\, ds = g(z,p), \quad z > h \qquad (3.15b)$$

In the above equations, the following abbreviations have been used

$$f(z,p) = \int_0^\infty t\, A(t,p) J_2(at) e^{-z\sqrt{t^2+p^2/c_1^2}}\, dt \qquad (3.16a)$$

$$g^*(z,p) = \int_0^\infty A(\theta,p) J_1(a\theta) e^{-z\sqrt{\theta^2+p^2/c_1^2}} d\theta + \frac{2G}{\pi} \int_0^\infty \frac{1}{\alpha_2} \frac{K_1(a\alpha_2)}{K_2(a\alpha_2)} \cdot$$
$$\cdot f_c(s,p) \cos(sz)\, ds \qquad (3.16b)$$

$$f_c(s,p) = \int_0^\infty f(z,p) \cos(sz)\, dz \qquad (3.16c)$$

$$H(s,p) = I_1(a\alpha_1) + G \frac{\alpha_1 I_2(a\alpha_1) K_1(a\alpha_2)}{K_2(a\alpha_2)} \qquad (3.16d)$$

$$G = G_1/G_2$$

With the help of equations (3.12), (3.15a) and (3.15c), $f_c(s,p)$ can be expressed as [reference--derivation of equation (2.22)]

$$f_c(s,p) = -\frac{\alpha_1 K_2(a\alpha_1)}{G_1}\int_o^b r\tau_o(r) I_1(r\alpha_1)\, dr \qquad (3.17)$$

Using this relation in equation (3.14), the last of the three unknown functions obtained as a result of the solution of differential equation, can be expressed as

$$C(s,p) = -G\left[\frac{2}{\pi} G_1 \int_o^b r\tau_o(r) I_1(r\alpha_1)\, dr \right. \\ \left. I_2(a\alpha_1) B(s,p)\right] \frac{\alpha_1 K_2(a\alpha_1)}{\alpha_2 K_2(a\alpha_2)} \qquad (3.18)$$

where $B(s,p)$ will be evaluated from the dual integral equations (3.15)

Solution of the Dual Integral Equations

The dual integral equations for the transient vibration defined by equations (3.15) have the same appearance as those derived for the steady-state vibration described in equations (2.21), except that the former are in the transformed plane. Therefore, the solution of equations (3.15) can readily be obtained following an identical procedure as delineated in Chapter 2 [reference--derivation of equations (2.24) to (2.36)]. The solution in the form of an auxiliary function and other intermediate functions, all in the transformed plane,

is as follows

$$B(s,p) = B^*(s,p) + B^{**}(s,p) \tag{3.19a}$$

$$B^*(s,p) = N(s,p)/H(s,p) \tag{3.19b}$$

$$N(s,p) = \int_0^h t^{\frac{1}{2}}\, \bar{\phi}(t,p) J_0(st)\,dt \tag{3.19c}$$

$$B^{**}(s,p) = \frac{2}{\pi}\frac{K_1(a\alpha_2)}{H(s,p)}\left\{\frac{1}{G_1} - \frac{\alpha_1 K_2(a\alpha_1)}{G_2\alpha_2 K_2(a\alpha_2)}\right\}\int_0^b rI_1(r\alpha_1)\tau_0(r)\,dr \tag{3.19d}$$

The auxiliary function $\bar{\phi}(t,p)$ is defined by the Fredholm equation of the second kind

$$\bar{\phi}(t,p) + \int_0^h \bar{\phi}(\theta,p)\, K(\theta,t,p)\,d\theta = t^{\frac{1}{2}} g(t,p) \tag{3.20a}$$

where

$$K(\theta,t,p) = (\theta t)^{\frac{1}{2}} \int_0^\infty s[F(s,p)-1]J_0(st)J_0(s\theta)\,ds \tag{3.20b}$$

$$F(s,p) = (1+G)\frac{I_2(as)}{H(s,p)} \tag{3.20c}$$

$$g(t,p) = \frac{-2(1+G)}{\pi}\int_0^\infty \left[\frac{\alpha_1 K_2(a\alpha_1)}{G_1} + \left\{\frac{1}{G_1}\frac{\alpha_1 K_2(a\alpha_1)}{G_2\alpha_2 K_2(a\alpha_2)}\right\}\cdot \alpha_1 I_2(a\alpha_1)\right.$$
$$\left.\frac{K_1(a\alpha_1)}{H(s,p)}\right] J_0(st)\left[\int_0^b rI_1(r\alpha_1)\tau_0(r)\,dr\right] ds \tag{3.20d}$$

Once the auxiliary function $\bar{\phi}(t,p)$ is determined numerically from equations (3.20), all physical quantities of interest including the stress intensity factor can be obtained by proper application of Laplace inversion theorem.

Stress-Intensity Factor

Similar to the steady-state vibration in Chapter 2, a square-root singularity of the time-dependent stress at the crack tip is also observed for transient vibration. Following an identical procedure [see equations (2.37) to (2.42)], the singular part of the shear stress at the crack tip can be obtained in the transform plane as [Fig.3]

$$\bar{\tau}_{r\theta_1}(a,h+\delta,p) = -\frac{G_1}{1+G}\,\frac{\bar{\phi}(h,p)}{p(2\delta)^{\frac{1}{2}}} + 0(\delta^{\circ})$$

Applying the Laplace inversion theorem, the time dependent stress becomes

$$\tau_{r\theta_1}(a,h+\delta,t) = -\frac{G_1}{1+G}\cdot\frac{1}{(2\delta)^{\frac{1}{2}}}\cdot\frac{1}{2\pi i}\int_{B_r}\bar{\phi}(h,p)\,\frac{e^{pt}}{p}\,dp + \ldots$$

where the dots indicate terms which are finite at the crack tip.

The dynamic stress intensity factor, $k_3(t)$ for the torsional mode can now be defined as

$$k_3(t) = -\frac{G_1}{1+G}\,\phi(h,t) \qquad (3.21a)$$

in which

$$\phi(h,t) = \frac{1}{2\pi i}\int_{Br}\bar{\phi}(h,p)\,\frac{e^{pt}}{p}\,dp \qquad (3.21b)$$

The auxiliary function $\bar{\phi}(h,p)$ can be obtained from the numerical solution of equations (3.20), a procedure which will be

discussed in Chapter 6 .

Examples

The same two examples used in Chapter 2 to illustrate the results, can also be considered for the transient vibration. Adopting identical procedure, it can be shown that the constant stress is related to the torque as

$$\tau_o(r) = k = \frac{3T}{2\pi b^3} \tag{3.24}$$

and the right-hand integral in the Fredholm equation is given by

$$g(t,p) = -\frac{T(1+G)}{2\pi^2 G_1}\int_o^\infty \alpha_1^2 \left[K_2(a\alpha_1) + \left\{1 - \frac{G\alpha_1 K_2(a\alpha_1)}{\alpha_2 K_2(a\alpha_2)}\right\} \cdot \right.$$

$$\left. \cdot\ \alpha_1 I_2(a\alpha_1)\frac{K_1(a\alpha_1)}{H(s,p)}\right] J_o(st)ds \tag{3.25}$$

Similarly, a linearly varying stress is related to the torque as

$$\tau_o(r) = \frac{\tau_o r}{b} = \frac{2rT}{\pi b^4} \tag{3.26}$$

and right-hand integral is

$$g(t,p) = -\frac{T(1+G)}{\pi b^4 G_1}\int_o^\infty \left[\alpha_1 K_2(a\alpha_1) + \left\{\frac{G\alpha_1 K_2(a\alpha_1)}{\alpha_2 K_2(a\alpha_2)}\right\} \cdot \right.$$

$$\left. \cdot\ \alpha_1 I_2(a\alpha_1)\frac{K_1(a\alpha_1)}{H(s,p)}\right] J_o(st) \left[\int_o^b r^2 I_1(r\alpha_1)dr\right]ds \tag{3.27}$$

In the above equations, T denotes the impulsive torque.

Knowing the right hand side of equation (3.20a) as determined by equations (3.23) and (3.27) above, the solution of the Fredholm integral equation (3.20) can be performed numerically in the p-plane to yield $\bar{\phi}(p)$ and consequently, equation (3.21b) yields the stress-intensity factor in the real plane. It is interesting to note that in this class of problems there is a peak in the value of k_3 over the first corresponding static case (by an amount of about 40%). After that k_3 oscillates about the static value. This is discussed in detail in chapter 6.

Chapter 4

STATIC TORSIONAL LOAD

The crack geometry shown in Fig. 1 and treated for dynamic loading in Chapters 2 and 3, is studied in this chapter under the application of a static torsional load. Noting that the static load is simply a special case of two previous dynamic loadings, the static solution can easily be recovered from solutions already obtained in Chapters 2 and 3, by letting either

$$\omega = 0$$

for the steady state vibration, or

$$p = 0$$

for the transient vibration.

In any case, the Fredholm equation reduces to [reference equations (2.34), (2.36) and (3.20)]

$$\phi(t) + \int_0^h \phi(\theta)\, k(\theta,t)\, d\theta = t^{\frac{1}{2}} g(t) \tag{4.1a}$$

where

$$k(\theta,t) = (\theta t)^{\frac{1}{2}} \int_0^\infty s\left[(1+G)\,\frac{I_2(as)}{H(s)} - 1\right] \cdot$$

$$\cdot\, J_0(\theta s)\, J_0(st)\, ds \tag{4.1b}$$

$$H(s) = I_1(as) + G\, I_2(as)\,\frac{K_1(as)}{K_2(as)} \tag{4.1c}$$

$$g(t) = -\frac{2(1+G)}{\pi G_1}\int_0^\infty s\left[K_2(as) + (1-G)\frac{I_2(as)K_1(as)}{H(s)}\right]\cdot$$

$$\cdot J_0(st)\left[\int_0^b r\, I_1(rs)\tau_0(r)dr\right]ds \qquad (4.1d)$$

and the static stress intensity factor for the torsional mode is expressed as

$$k_3 = -\frac{G_1}{1+G}\phi(h) \qquad (4.2)$$

where $\phi(h)$ is the solution of the above Fredholm equation at the crack tip.

For a constant specified stress distribution, g(t) can be further simplified to

$$g(t) = -\frac{T(1+G)}{2\pi^2 G_1}\int_0^\infty s^2\left[K_2(as) + (1-G)I_2\frac{I_2(as)K_1(as)}{H(s)}\right]\cdot$$

$$\cdot J_0(st)\, ds$$

where T is the static torque applied on the plane z = 0.

For a linearly varying stress distribution, g(t) is given by

$$g(t) = \frac{-T(1+G)}{\pi^2 b^4 G}\int_0^\infty s^2\left[K_2(as) + (1-G)\frac{I_2(as)K_1(as)}{H(s)}\right]\cdot$$

$$\cdot J_0(st)\left[\int_0^b r^2 I_1(rs)dr\right]ds$$

where b is the radius of the circular region over which the torque is applied.

It is clear from the above that considerable analytical simplification occurs in the static case. However, the integral equation governing the function (eqation 4.1a) still has to be solved numerically to determine the physical quantities of interest. The numerical solution of the Fredholm equation and the corresponding variation of the static stress-intensity factor, due to a concentrated torque with material and geometric parameters, is discussed in detail in Chapter 6.

Chapter 5

STEADY-STATE TORSIONAL VIBRATION OF A LAYER

The steady-state torsional vibration of a layer is considered in this chapter (Fig. 2). The inner cylinder is surrounded by different material of large diameter, but both media have a finite thickness (d). A finite cylindrical crack of depth h ($h < d$) exists at the interface of the two media.

The steady-state solution obtained in chapter 2 is applied to this problem with an appropriate modification to account for finiteness of the depth in lieu of a half-space. Boundary conditions lead to a set of dual-series equations which are solved to yield a Fredholm integral equation of the second kind. The stress-intensity factor, k_3, is obtained in terms of the auxiliary function of the Fredholm equation.

Basic Equations and Formulations

Adopting the same procedure of Chapter 2 and Appendix A, with appropriate modification for the finite layer, the only non-vanishing displacement component in each medium can be written as

$$u^*_{\theta_1}(r,z) = \int_0^\infty [A(s)e^{-\alpha_1 z} + D(s)e^{\alpha_1 z}]J_1(rs)ds + \sum_{n=0}^{\infty} B_n I_1(r\sqrt{s_n^2-\omega^2\rho_1/G_1})\cos(s_n z) \qquad (5.1a)$$

$$u^*_{\theta_2}(r,z) = \sum_{n=0}^{\infty} C_n K_1(r\sqrt{s_n^2-\omega^2\rho_2/G_2})\cos(s_n z) \qquad (5.1b)$$

where

$$\alpha_1 = \sqrt{s^2 - \omega^2 \rho_1 / G_1}$$

having a branch-cut for $s < \omega^2 \rho_1 / G_1$ as discussed by Noble [34].

The unknown variables A(s), D(s), B_n, C_n, and S_n (n=0,1,2,...∞) are obtained from the boundary conditions. Note that for large r, K_1 dies out quickly and thus there will be no inward waves. At the stress free boundary (z=d), the waves will be reflected.

Boundary Conditions

In addition to the boundary condition of equations (2.11) and (2.12), assume the remote surface of the layer to be stress-free, i.e.

$$\tau_{\theta z_1}(r,d) = \tau_{\theta z_2}(r,d) = 0 \qquad (5.2)$$

which requires the following conditions:

$$\int_0^\infty \alpha_1 [-A(s) e^{-\alpha_1 d} + D(s) e^{\alpha_1 d}] J_1(rs)\, ds = 0$$

$$\text{i.e. } D(s) = A(s) e^{-2\alpha_1 d} \qquad (5.3a)$$

$$\text{and} \quad S_n = n\pi/d, \ n = \text{integer} \qquad (5.3b)$$

For simplicity of algebraic work, the depth of the layer can be assumed to be equal to π without affecting the generality of the problem. Therefore, equations (5.3) can be simplified as follows:

$$D(s) = A(s)e^{-2\alpha_1\pi} \tag{5.4a}$$

$$s_n = n, \quad n=0,1,2,\ldots\infty \tag{5.4b}$$

Introducing the followint notation

$$\lambda_{n_i} = \sqrt{n^2-\omega^2\rho_i/G_i}, \quad i = 1,2$$

the stress-displacement field in two media can be written from equations (5.1).

In the inner medium ($0 \leq r \leq a$, $0 \leq z \leq \pi$)

$$u^*_{\theta_1}(r,z) = \int_0^\infty A(s)\,[e^{-\alpha_1 z}+e^{\alpha_1(z-2\pi)}]J_1(rs)\,ds + \sum_{n=0}^{\infty} B_n I_1(r\lambda_{n1})\cos(nz) \tag{5.5a}$$

$$\frac{I}{G_1}\tau^*_{r\theta_1}(r,z) = -\int_0^\infty sA(s)\,[e^{-\alpha_1 z}+e^{\alpha_1(z-2\pi)}]J_2(rs)\,ds + \sum_{n=0}^{\infty} \lambda_{n1}\, I_2(r\lambda_{n1})\cos(nz) \tag{5.5b}$$

$$\frac{1}{G_1}\tau^*_{\theta z_1}(r_1 z) = \int_0^\infty \alpha_1 A(s)\,[-e^{-\alpha_1 z} + e^{\alpha 1(z-2\pi)}\,[J_1(rs)\,ds - \sum_{n=0}^{\infty} n\, B_n\, I_1(r\lambda_{n_1})\sin(nz) \tag{5.5c}$$

while in the outer medium ($a \leq r \leq \infty$, $0 \leq z \leq \pi$)

$$u^*_{\theta_2}(r,z) = \sum_{n=0}^{\infty} C_n K_1(r\lambda_{n2})\cos(nz) \tag{5.6a}$$

$$\frac{1}{G_2}\tau^*_{r\theta_2}(r,z) = -\sum_{n=0}^{\infty} \lambda_{n_2} C_n K_2(r\lambda_{n_2}) \cos(nz) \qquad (5.6b)$$

$$\frac{1}{G_2}\tau_{\theta z_2}(r,z) = -\sum_{n=0}^{\infty} n\, C_n K_1(r\,\lambda_{n_2}) \sin(nz) \qquad (5.6c)$$

Application of the bounding condition on z = 0 plane [see equation (2.12a)] yields A(s) in terms of the specified stress

$$A(s) = \frac{1}{G_1\alpha_1(-1+e^{-2\alpha,\pi})} \int_o^{\infty} r\, \tau_o(r) J_1(rs)\, ds \qquad (5.7)$$

The traction-free condition on the crack surface [see equation (2.12b)] supplies the following relations for $0 \lesssim z \lesssim h$

$$\sum_{n=0}^{\infty} \lambda_{n_1} B_n I_2(a\lambda_{n_1}) \cos(nz) = \int_o^{\infty} sA(s)\left[e^{-\alpha_1 z} + e^{\alpha_1(z-2\pi)}\right] J_2(as)\, ds \qquad (5.8a)$$

$$\sum_{n=0}^{\infty} \lambda_{n_2} C_n K_2(a\,\lambda_{n_2}) \cos(nz) = 0 \qquad (5.8b)$$

while the continuity conditions on the bond surface [see equations (2.12c) and (2.12d)] provide the following additional relations for $h \lesssim z \lesssim \pi$

$$\sum_{n=0}^{\infty} [B_n I_1(a\lambda_{n_1}) - C_n K_1(a\lambda_{n_2})] \cos(nz) = -\int_{\delta}^{\infty} A(s)\left[e^{-\alpha_1 z} + e^{\alpha_1(z-2\pi)}\right] J_1(as)\, ds \qquad (5.8c)$$

$$\sum_{n=0}^{\infty} [G_1 \lambda_{n_1} B_n I_2(a\lambda_{n_1}) + G_2 \lambda_{n_2} C_n K_2(a\lambda_{n_1})] \cos(nz)$$

$$= G_1 \int_0^{\infty} sA(s)[e^{-\alpha,z} + e^{\alpha_1(z-2\pi)}] \qquad (5.8d)$$

Equations (5.8a), (5.8b) and (5.8d) can be algebraically combined and further manipulated to provide the following relation:

$$\sum_{n=0} [\lambda_{n_1} B_n I_2(a\lambda_{n_1}) + \frac{1}{G} \lambda n_2 C_n K_2(a\lambda n_2) \cos(nz) = f(z),$$

$$0 \leq z \leq \pi, \; G_1 \neq 0 \qquad (5.9a)$$

where

$$f(z) = \int_0^{\infty} s\, A(s)[e^{-\alpha_1 z} + e^{\alpha_1(z-2\pi)}] J_2(as)\, ds) \qquad (5.9b)$$

By the application of Fourier series cosine transform, equation (5.9a) can be written as

$$\lambda_{0_1} B_o I_2(a\lambda_{o_1}) + \frac{1}{G} \lambda_{o_2} C_o K_2(a\lambda_{o_2}) = \frac{1}{\pi} \int_o^{\pi} f(z)\, dz \qquad (5.10a)$$

$$\lambda_{n_1} B_n I_2(a\lambda_{n_1}) + \frac{1}{G} \lambda_{n_2} C_n K_2(a\lambda_{n_2}) = \frac{2}{\pi} \int_o^{\pi} f(z) \cos(nz)\, dz, \; n=1,2,. \qquad (5.10b)$$

where C_0 and C_n are readily obtained as

$$C_o = \frac{G}{\lambda_{o_2} K_2(a\lambda_{o_2})} [\frac{1}{\pi} \int_o^{\pi} f(z)\, dz - \lambda_{0_1} I_2(a\lambda_{0_1}) B_0] \qquad (5.11a)$$

$$C_n = \frac{G}{\lambda_{n_2} K_2(a\lambda_{n_2})} [\frac{2}{\pi} \int_o^{\pi} f(z) \cos(nz)\, dz - \lambda_{n_1} I_2(a\lambda_{n_1}) B_n], \; n=1,2,... \qquad (5.11b)$$

The following dual series equations result by eliminating C_n from equation (5.8c) with the help of equations (5.11) and regrouping with equation (5.8a)

$$\sum_{n=0}^{\infty} \lambda_{n_1} B_n I_2(a\lambda_{n_1}) \cos(nz) = f(z), \quad 0 \leq z \leq h \tag{5.12a}$$

$$\sum_{n=0}^{\infty} B_n H_n \cos(bz) = g^*(z), \quad z > h \tag{5.12b}$$

in which the following additional abbreviations have been adopted

$$H_o = I_1(a\lambda_{0_1}) + G \frac{\lambda_{o_1} I_2(a\lambda_{0_1}) K_1(a\lambda_{0_2})}{\lambda_{o_2} K_2(a\lambda_{0_2})} \tag{5.12c}$$

$$H_n = I_1(a\lambda_{n_1}) + G \frac{\lambda_{n_1} I_2(a\lambda_{n_1}) K_1(a\lambda_{n_2})}{\lambda_{n_2} K_2(a\lambda_{n_2})}, \quad n=1,2,\ldots \tag{5.12d}$$

$$g^*(z) = -\int_0^{\infty} A(\theta)\left[e^{-\alpha_1 z} + e^{\alpha(z-2\pi)}\right] J_1(a\theta)\, d\theta + \frac{G}{\pi} \sum_{n=0}^{\infty} \frac{K_1(a\lambda_{n_2})}{\lambda_{n_2} K_2(a\lambda_{n_2})} f_n \tag{5.12e}$$

where

$$f_n = \begin{cases} \int_0^{\pi} f(z)\, dz, & n = 0 \\ \int_0^{\pi} f(z) \cos(nz)\, dz, & n = 1,2,\cdots \end{cases} \tag{5.12f}$$

Solution of Dual Series Equations

As in Chapter 2, express B_n as a summation of two new functions:

$$B_n = B_n^* + B_n^{**} \tag{5.13a}$$

where

$$\sum_{n=0}^{\infty} B_n^{**} H_n \cos(nz) = g^*(z), \quad 0 \leq z \leq \pi \tag{5.13b}$$

By Fourier cosine transform, it follows

$$B_o^{**} H_o = \frac{1}{\pi} \int_0^{\infty} g^*(z)dz \tag{5.14a}$$

$$B_n^{**} H_n = \frac{2}{\pi} \int_0^{\infty} g^*(z) \cos(nz)dz, \quad n=1,2,... \tag{5.14b}$$

Applying above relations on the dual series equations (5.12), one obtains

$$\sum_{n=0}^{\infty} \lambda_{n1} (B_n^* + B_n^{**}) I_2(a\lambda_{n1}) \cos(nz) = f(z), \quad 0 \leq z \leq h \tag{5.15a}$$

$$\sum_{n=0}^{\infty} B_n^* H_n \cos(nz) = 0, \quad z > h \tag{5.15b}$$

Replacing B_n^* by a new function

$$\begin{aligned} N_n &= B_n^* H_n, \quad n = 1,2,... \\ \tfrac{1}{2}N_o &= B_o^* H_o \end{aligned} \tag{5.16}$$

and performing some algebraic manipulation, equations (5.15) can

be expressed as follows

$$(1+G)\ \frac{\lambda_{0_1} I_2(a\lambda_{0_1})}{2H_o}\ N_o + \sum_{n=0}^{\infty} n\ N_n \cos(nz)$$

$$= (1+G)W(z) + \sum_{n=0}^{\infty} n(1-F_n)N_n \cos(nz),\ 0 \leq z \leq h \qquad (5.17a)$$

$$\frac{1}{2} N_o + \sum_{n=1}^{\infty} N_n \cos(nz) = 0,\quad z > h \qquad (5.17b)$$

The following abbreviations have been introduced in above derivation

$$W(z) = f(z) - \sum_{n=0}^{\infty} \lambda_{n_1} B_n^{**} I_2(a\lambda_{n_1})\cos(nz) \qquad (5.17c)$$

$$F_n = \frac{\lambda n_1}{nH_n} I_2(a\lambda_{n_1}) \qquad (5.17d)$$

In order to solve the dual series equations, introduce an auxiliary function $\phi^*(t)$ such that

$$N_n = \int_o^h \phi^*(t) J_o(nt)dt,\ n = 1,2,... \qquad (5.18)$$

$$N_o = \int_o^h \phi^*(t)dt \qquad (5.18)$$

Note that equation (5.17b) is automatically satisfied by the above definition of the auxiliary function.

Equation (5.17a) can now be expressed in terms of $\phi^*(t)$ with the help of equation (5.18) as follows:

$$\frac{d}{dz}\int_o^h \phi^*(t)\left[\sum_{n=1}^{\infty}\sin(nz)J_o(nt)\right]dt$$

$$= -\frac{(1+G)\lambda_{0_1} I_2(a\lambda_{01})}{2H_o} N_o + (1+G)W(z)$$

$$+\sum_{n=1}^{\infty} n(1-F_n)N_n \cos(nz),\ 0 \leq z \leq h \qquad (5.19)$$

Making use of the following identity [23]

$$\sum_{n=1}^{\infty}\sin(nz)J_o(nt) = \frac{H(z-t)}{\sqrt{z^2-t^2}} - \frac{1}{\pi}\int_o^{\infty}\frac{e^{-\xi}}{\sin h\xi} I_o(\xi t)\sin h(\xi z)d\xi$$

where H(z-t) is a Heaviside function, and integrating separately between two different intervals, namely 0 to z and z to h, equation (5.19) can be written as

$$\frac{d}{dz}\int_o^z \frac{\phi^*(t)dt}{\sqrt{z^2-t^2}} - \frac{1}{\pi}\frac{d}{dz}\int_o^h \phi^*(t)\left[\int_o^{\infty}\frac{e^{-\xi}I_o(\xi t)\sin h(\xi z)d\xi}{\sin h\xi}\right.$$

$$= -(1+G)\frac{\lambda_{0_1} I_2(a\lambda_{o_1})}{2H_o} N_o + (1+G)W(z) + \sum_{n=1}^{\infty} n(1-F_n)N_n \cos(nz) \qquad (5.20)$$

Making use of the following Abel integral solution,

$$\frac{d}{dz}\int_o^z \frac{\phi^*(t)dt}{\sqrt{z^2-t^2}} = f(z) \qquad (5.21a)$$

$$\phi^*(t) = \frac{2}{\pi} t \int_o^h \frac{f(z)}{\sqrt{t^2-z^2}} \qquad (5.21b)$$

equation (5.20) can be transformed to a standard Fredholm equation of the second kind as follows:

$$\phi^*(t) + t\int_0^h K(\eta,t)\phi^*(\eta)d\eta = \frac{2(1+G)}{\pi}\, t\int_0^t \frac{W(z)}{\sqrt{t^2-z^2}}dz \qquad (5.22a)$$

where the kernel is

$$K(\eta,t) = -\frac{1}{n}\int_0^\infty \frac{\xi e^{-\xi} I_o(\xi\eta) I_o(\xi t)}{\sin h\xi}d\xi + (1+G)\frac{\lambda_o I_2(a\lambda_{o1})}{2H_o}$$

$$-\frac{2}{\pi}\sum_{n=1}^{\infty} n(1-F_n)J_o(n\eta)J_o(nt) \qquad (5.22b)$$

The following identities have been used to arrive at the above solution

$$\int_0^t \frac{\cos(nz)}{\sqrt{t^2-z^2}}dz = \frac{\pi}{2} J_o(nt)$$

$$\int_0^t \frac{\cosh(nz)}{\sqrt{t^2-z^2}}\, dz = \frac{\pi}{2} I_o(nt)$$

For ease of comparison with the results obtained in Chapter 2, redefine $\phi^*(t)$ as

$$\phi^*(t) = t^{\frac{1}{2}}\phi(t) \qquad (5.23)$$

so that the above Fredholm equastion takes the form

$$\phi(t) + \int_0^h \phi(\Theta)K(\Theta,t)d\Theta = t^{\frac{1}{2}}g(t) \qquad (5.24a)$$

where

$$K(\theta,t) = (\theta t)^{\frac{1}{2}}\left[-\frac{1}{\pi}\int_0^\infty \frac{\xi e^{-\xi} I_0(\xi\theta) I_0(\xi t) d\xi}{\sin h\xi} + (1+G)\frac{\lambda_{01} I_2(a\lambda_{01})}{2H_0} - \frac{2}{\pi}\sum_{n=1}^{\infty} n(1-F_n) J_0(n\theta) J_0(nt)\right] \tag{5.24b}$$

$$g(t) = \frac{2}{\pi}(1+G)\, t^{\frac{1}{2}} \int_0^t \frac{W(z)}{\sqrt{t^2-z^2}}\, dz \tag{5.24c}$$

Note that for a specified stress $\tau_0(r)$, $g(t)$ is a known function, and the unknown auxiliary function $\phi(t)$ can easily be numerically solved from equation (5.24a).

Stress-Intensity Factor

Following an identical procedure as used in Chapter 2, the possible singular part of the shear stress can be extracted and expressed in terms of $\phi(t)$ as

$$\tau^*_{r\theta_1}(a,z) = \frac{G_1}{1+G} h^{\frac{1}{2}} \phi(h) \sum_{n=1}^{\infty} J_1(nh)\cos(nz) + \ldots, \quad z > h \tag{5-25}$$

Making use of the identity

$$\sum_{n=1}^{\infty} J_1(nh)\cos(nz) = \frac{1}{h}\left[1 - \frac{zH(z-h)}{\sqrt{z^2-h^2}}\right]$$

and proceeding as in Chapter 2 [see equations (2.41) and (2.42)] the singular term of the time dependent shear stress can be expressed as

$$[\tau_{r\theta_1}]_{\substack{r=a \\ z=h+\delta}} = -\frac{G_1}{1+G}\frac{\phi(h)}{\sqrt{2\delta}} H(\delta)\cos(\omega t) + 0(\delta^0) \tag{5.26}$$

Therefore, by definition, the dynamic stress-intensity factor is as follows:

$$k_3 = - \frac{G_1}{1+G} \phi(h) \tag{5.27}$$

where $\phi(h)$ is the solution of Fredholm equation (5.24a).

The numerical solutions of $\phi(h)$ and k_3 for the above equations are similar to those in equations (2.36) and (2.42). The latter have been solved in detail in Chapter 6, and similar qualitative results are expected for the layer. Since the layer has a stress-free boundary, it is expected that the static local stress will increase with the decreasing distance between the free boundary and the crack [4]. For the dynamic factor k_3, a peak will occur but possibly with a different magnitude of amplification.

Chapter 6

NUMERICAL SOLUTION AND COMPUTATION OF STRESS-INTENSITY FACTOR

In this chapter, the numerical solution of the Fredholm equations obtained in Chapters 2, 3 and 4, is discussed in some detail. The quantity of physical interest, namely the stress-intensity factor which is known to control the propagation of the crack, is computed numerically for different values of material properties, crack geometry and shear wave frequency. The numerical treatments of the steady-state and transient vibrations are discussed separately in two sections of this chapter.

Steady-State Vibrations

For numerical integration, it is convenient to express the Fredholm equation in equations (2.36) in terms of dimensionless parameters. The following notations are introduced and made use of in solving the example of a concentrated torque (example 1 of page 37)

$$t = h\xi \tag{6.1a}$$

$$\theta = h\eta \tag{6.1b}$$

$$s = \lambda/h \tag{6.1c}$$

$$a = \bar{a}h \tag{6.1d}$$

$$\alpha_i \equiv \left(s^2 - \frac{\omega^2\rho_1}{G_1}\right)^{\frac{1}{2}} = \left(\frac{\lambda^2}{h^2} - \frac{\omega^2\rho_i}{G_i}\right)^{\frac{1}{2}} = \frac{\gamma_i}{h} \tag{6.1e}$$

$$\phi(t) \equiv \phi(h\xi) = \frac{T(1+G)\sqrt{h}}{2\pi^2 h^3 G_1}\,\Phi(\xi) \tag{6.1f}$$

so that equations (2.36) assume the nondimensional form

$$\Phi(\xi) + \int_0^1 \Phi(\eta) L(\eta,\xi)\, d\eta = \xi^{\frac{1}{2}}\, M(\xi) \tag{6.2a}$$

where the symmetrical kernel is

$$L(\eta,\xi) = (\xi\eta)^{\frac{1}{2}} \int_0^\infty \lambda\left[(1+G)\,\frac{\gamma_1 I_2(\bar{a}\gamma_1)}{\lambda H(\lambda)} - 1\right] \cdot J_0(\lambda\xi)\, J_0(\lambda\eta)\, d\lambda \tag{6.2b}$$

and

$$M(\xi) = -\int_0^\infty \gamma_1^2 \left[K_2(\bar{a}\gamma_1) + \left\{1 - \frac{G\gamma_1 K_2(a\gamma_1)}{\gamma_2 K_2(a\gamma_2)}\right\} I_2(\bar{a}\gamma_1) \cdot \frac{K_1(\bar{a}\gamma_1)}{H(\lambda)}\right] J_0(\lambda\xi)\, d\lambda \tag{6.2c}$$

Using the new definition of the auxiliary function in equastion (6.1), the stress-intensity factor for the steady-state vibration defined in equation (2.42) can be expressed in terms of $\Phi(\xi)$ as

$$k_3 = -\frac{T\sqrt{h}}{2\pi^2 h^3}\,\Phi(1) \tag{6.3}$$

Numerical solutions of the Fredholm equation (6.2a) are obtained for various physical parameters by following the Kantorvich and Krylov method [27] which basically replaces the integral equation with a system of simultaneous algebraic equations that can easily be solved with the aid of a digital computer. However, in the study of the kernel, a few problems

are encountered in the numerical work. These problems and their respective remedies are discussed in the sequel.

First, the integrand of the kernel given by equation (6.2b) converges very slowly, requiring a great amount of computer time. This behavior can be improved by separating the slowly convergent part from the rapidly convergent part of the integrand, and obtaining a "close form" solution of the slowly convergent part.

For large values of the argument, the following expansions of the Bessel functions can be used [25]

$$I_1(x) = \frac{e^x}{\sqrt{2\pi x}} \left[1 - \frac{3}{8x} - \frac{15}{128x^2} + \ldots\right]$$

$$I_2(x) = \frac{e^x}{\sqrt{2\pi x}} \left[1 - \frac{15}{8x} + \frac{105}{128x^2} - \ldots\right]$$

$$K_1(x) = \sqrt{\frac{\pi}{2x}}\, e^{-x}\left[1 + \frac{3}{8x} - \frac{15}{128x^2} + \ldots\right]$$

$$K_2(x) = \sqrt{\frac{\pi}{2x}}\, e^{-x}\left[1 + \frac{15}{8x} + \frac{105}{128x^2} - \ldots\right]$$

Therefore, for large values of x, the following relations are obtained

$$I_1(x)K_2(x) = \frac{1}{2x}\left[1 + \frac{3}{2x} + 0(x^{-2})\right]$$

$$I_2(x)K_2(x) = \frac{1}{2x}\left[1 + 0(x^{-2})\right]$$

$$I_2(x)K_1(x) = \frac{1}{2x}\left[1 - \frac{3}{2x} + 0(x^{-2})\right]$$

Using these results, it can be shown that for large values of λ

$$\frac{(1+G)\gamma_1 I_2(\bar{a}\gamma_1)}{\lambda H(\lambda)} - 1 = \frac{G-1}{G+1}\frac{3}{2\bar{a}\lambda} + 0(\lambda^{-2})$$

which indicates that for G=1 (homogeneous case) the kernel is well behaved, and when $G \neq 1$, it has a removable singularity at the upper limit. Noting that for high values of λ

$$\gamma_1 \doteq \gamma_2 \doteq \lambda$$

and introducing the abbreviations

$$F(\gamma_1) = (1+G)\frac{\gamma_1 I_2(\bar{a}\gamma_1)}{\lambda H(\lambda)} \tag{6.4a}$$

$$F^*(\lambda_1) = \frac{G-1}{G+1}\quad\frac{3}{2\bar{a}\lambda} \tag{6.4b}$$

the logarithmic singularity at the upper limit can be seperated, and the kernel in equation (6.2b) can be split into two parts as

$$L(\eta,\xi) = (\xi\eta)^{\frac{1}{2}}\int_0^{\infty}\lambda F^*(\lambda_1)J_0(\lambda\xi)J_0(\lambda\eta)d\lambda + (\eta\xi)^{\frac{1}{2}}\int_0^{\lambda_0}\lambda\,[F(\gamma_1) - F^*(\lambda) - 1]\cdot J_0(\lambda\xi)J_0(\lambda\eta)d\lambda \tag{6.5}$$

In the above equation, λ_0 is chosen to be large enough to satisfy the following relation

$$F(\gamma_1) - 1 = F^*(\lambda_0)$$

Using the value of $F^*(\lambda)$ from equation (6.4b) and noting the identity [23]

$$\int_0^\infty J_0(\lambda\xi)J_0(\lambda\eta)\,d\lambda = \begin{cases} \frac{2}{\pi\xi}\,\kappa(\frac{\eta}{\xi}), & \xi > \eta \\ \frac{2}{\pi\eta}\,\kappa(\frac{\xi}{\eta}), & \xi < \eta \end{cases}$$

the kernel can be conveniently expressed as

$$L(\eta,\xi) = (\xi\eta)^{\frac{1}{2}}\left\{ \frac{3}{\pi\bar{a}}\,\frac{G-1}{G+1} \begin{bmatrix} \frac{1}{\xi}\,\kappa(\eta/\xi), & \xi > \eta \\ \frac{1}{\eta}\,\kappa(\xi/\eta), & \xi < \eta \end{bmatrix} \right.$$

$$+\int_0^{\lambda_0} \lambda\left[(1+G)\,\frac{\gamma_1 I_2(\bar{a}\gamma_1)}{\lambda\, H(\lambda)} - \frac{G-1}{G+1}\quad\frac{3}{2\bar{a}\lambda} - 1\right]\cdot$$

$$\left.\cdot\, J_0(\lambda\xi)J_0(\lambda\eta)\,d\lambda\right\} \qquad (6.6)$$

In above equations, $\kappa(x)$ denotes the standard elliptic integral of the first kind. It is observed that the integrand of the second expression in equation (6.6) converges within a reasonable limit and at a much faster rate than that of equation (6.2b).

The second unusual problem encountered during the numerical process is that when the Fredholm equation (6.2a) is replaced by a system of simultaneous equations [see equation (6.8) where $i = 1,2,\ldots(2n+1)$; $j = 1,2,\ldots(2n+1)$], the kernel in equation (6.6) becomes indeterminate for $i = j$, i.e. for $\eta = \xi$. This problem can be overcome by the use of a modified method of integration suggested by Kantorvich and Krylov [27]. Basically, this method consists of rewriting the Fredholm equation (6.2a) in the following form

$$\Phi(\xi)[1 + L^*(\xi)] + \int_0^1 L(\eta,\xi)[\Phi(\eta) - \Phi(\xi)]d\eta = \xi^{\frac{1}{2}}M(\xi) \qquad (6.7a)$$

in which

$$L^*(\xi) = \int_0^1 L(\eta,\xi)d\eta \qquad (6.7b)$$

Replace the above equation by a system of simultaneous equations as follows:

$$\Phi_i[1 + L_i^* - \frac{1}{\Delta}\sum_{j=1}^{2n+1} A_j L_{ij}] + \frac{1}{\Delta}\sum_{j=1}^{2n+1} A_j L_{ij}\Phi_j = (\xi_i)^{\frac{1}{2}} M_i - \varepsilon_i, \quad i=1,2,\ldots(2n+1) \qquad (6.8)$$

where the following notations are used

$\Delta = \frac{1}{2n}$

$\xi_i = (i-1)\,\Delta$

$\eta_j = (j-1)\,\Delta$

$A_1 = A_{2n+1} = 1/3,\ A_2 = A_4 = \ldots = 4/3,\ A_3 = A_5 = \ldots = 2/3$

[Simpson's Co-efficient]

$\Phi_i = \Phi(\xi_i)$

$L^*_i = L^*(\xi_i)$

$M_i = M(\xi_i)$

$$L_{ij} = \begin{cases} \frac{1}{2}[L(\xi_i,\eta_{i-1}) + L(\xi_i,\eta_{i+1})], & i = j \\ L(\xi_i,\eta_j), & i \neq j \end{cases}$$

ε_i = Numerical integration error which can be brought to a very small value by increasing the number of equations and, therefore, can be neglected.

Now, following reference [27], the diagonal terms (i.e. for i = j) of the matrix formed by equation (6.8) can be written as

$$L_{ij}(\Phi_j - \Phi_i) = \xi_x L(\xi_i, \eta_{i-1})[\Phi_{i-1} - \phi_i] + \xi_y L(\xi_i, \eta_{i+1})[\Phi_{i+1} - \Phi_i]$$

in which

$$\xi_x = \frac{\xi_{i+1} - \xi_i}{\xi_{i+1} - \xi_{i-1}}$$

$$\xi_y = \frac{\xi_i - \xi_{i-1}}{\xi_{i+1} - \xi_{j-1}}$$

Choosing equal intervals, ξ_x and ξ_y can be made equal to ½. Therefore, the i^{th} equation can be written as

$$\begin{aligned}
&\frac{1}{\Delta}\Phi_1 A_1 L_{i,1} + \frac{1}{\Delta}\Phi_2 A_2 L_{i,2} + \cdots \\
&+ \frac{1}{\Delta}\Phi_{i-1}(A_{i-1} + \xi_x)L_{i,i-1} + \Phi_i\left[1 + L_i^* - \frac{1}{\Delta}\sum_{j=1}^{i-1} A_j L_{ij}\right. \\
&\left. - \frac{1}{\Delta}\sum_{j=i+1}^{2n+1} A_j L_{ij} + \frac{1}{\Delta} A_i(-\xi_x L_{i,i-1} - \xi_y L_{i,i+1})\right] \\
&+ \frac{1}{\Delta}\Phi_{i+1}(A_{i+1} + \xi_y)L_{i,i+1} + \cdots \\
&+ \frac{1}{\Delta}\Phi_{2n+1} A_{2n+1} L_{i,2n+1} = (\xi_i)^{\frac{1}{2}} M_i
\end{aligned} \tag{6.9}$$

It must be emphasized, at this point, that in equation (6.9) Φ_i, L_{ij} and M_i are all complex variables because of the

complex nature of the term γ_i for $\lambda^2 < \frac{\omega^2 \rho_i}{G_i}$ [see equation (5.1e)]. This requires the solution of the Fredholm equation to be obtained using complex arithmetic. Unlike the vibration problem of a penny-shaped crack [15], the kernel $L(\eta,\xi)$ and the right-hand term $M(\xi)$ of equations (5.2) are too involved algebraically to be separated into real and imaginary parts easily. Each element of the matrices of equation (5.8) is complex in general. To this end, the following procedure is adopted to overcome the numerical problem.

The complex variable programming technique is employed and the numerical integration scheme is adopted to determine by computer the numerical value of each complex element of matrices formed by equation (6.8). These elements are further processed in the computer and decomposed into real and imaginary parts. Abbreviating each complex element of the left side of equation (5.9) by K_C, and the corresponding real and imaginary terms by K_R and K_I, the following decomposed equation can be written

$$(K_R + i\,K_I)_{i,1}\,(\Phi_R + i\,\Phi_I)_1 + \ldots$$
$$+(K_R + i\,K_I)_{i,j}\,(\Phi_R + i\,\Phi_I)_j + \ldots$$
$$+(K_R + i\,K_I)_{i,N}\,(\Phi_R + i\,\Phi_I)_N = (\xi_i)^{\frac{1}{2}}(M_R + iM_I)_i$$
$$i = 1,2,\ldots N$$

in which the following complex identities are used

$$\Phi_i = (\Phi_R + i\Phi_I)_i$$

$$M_i = (M_R + i\, M_I)_i$$

$$K_C = K_R + i\, K_I$$

Equating the real and the imaginary parts separately, and rearranging the terms, the following equations are obtained

$$(K_R)_{i,1}\,(\Phi_R)_1 + \ldots + (K_R)_{i,j}\,(\Phi_R)_j + \ldots + (K_R)_{i,N}(\Phi_R)_N$$
$$-(K_I)_{i,1}\,(\Phi_I)_1 - \ldots - (K_I)_{i,j}\,(\Phi_I)_j - \ldots - (K_I)_{i,N}(\Phi_I)_N$$
$$= (\xi_i)^{\frac{1}{2}}\,(M_R)_i$$

and

$$(K_I)_{i,1}(\Phi_R)_1 + \ldots + (K_I)_{i,j}\,(\Phi_R)_j + \ldots + (K_I)_{i,N}(\Phi_I)_N$$
$$+(K_R)_{i,1}(\Phi_I)_1 + \ldots + (K_R)_{i,j}\,(\Phi_I)_j + \ldots + (K_R)_{i,N}(\Phi_I)_N$$
$$= (\xi_i)^{\frac{1}{2}}\,(M_I)_i$$
$$i = 1,2,\ldots N$$

It must be noted that the original kernel matrix of N x N dimension is now increased to the size of 2N x 2N when both the above equations are combined. Since the required computer (CPU) time increases rapidly with the values of N, several such values are tried to search for a reasonable number without comprising accuracy. It is found that values of N larger than 19 yield no appreciable difference in results. Therefore, all Fredholm equations are solved for N = 19.

The decomposition into real and imaginary parts, and

rearrangement of elements to form the new matrix, as described above, are processed in the computer writing appropriate programs. Finally, the 2N number of simultaneous equations are solved in the computer adopting the standard procedure for matrix method of solution, and the stress-intensity factor is obtained using equation (6.3) after extracting the real values of the auxiliary function Φ at the crack tip. Such complete solutions are obtained for various material properties, crack geometrics and wave number of shear wave propagation, and the results are displayed graphically in Figures 4,5 and 6.

Fig. 4 exhibits the effect of wave number (i.e. indirectly the frequency) of the impingent torsional wave on the stress-intensity factor for various modulus-ratios. The normalized dynamic k_3 increases with the wave number, reaches a maximum, and then rapidly decreases. The static k_3 is readily obtained at zero value of the wave number. For G = 3, the dynamic amplification is about 1.9 at a wavelength of about 90% of the crack depth. Larger G-values result in less stress-intensity factors, but with a greater relative dynamic amplification at a smaller wave length. For large wave numbers, the crack plane approximates the stress-free surface of a half-space, and k_3 for a higher G-value vanishes at a lower wavelength. However, k_3, by definition, never attains a negative value. The curves in Fig. 4 are obtained for a/h = 1.

Figs. 5 and 6 show the effect of variation of shear modulus and crack radius on the static stress-intensity factor.

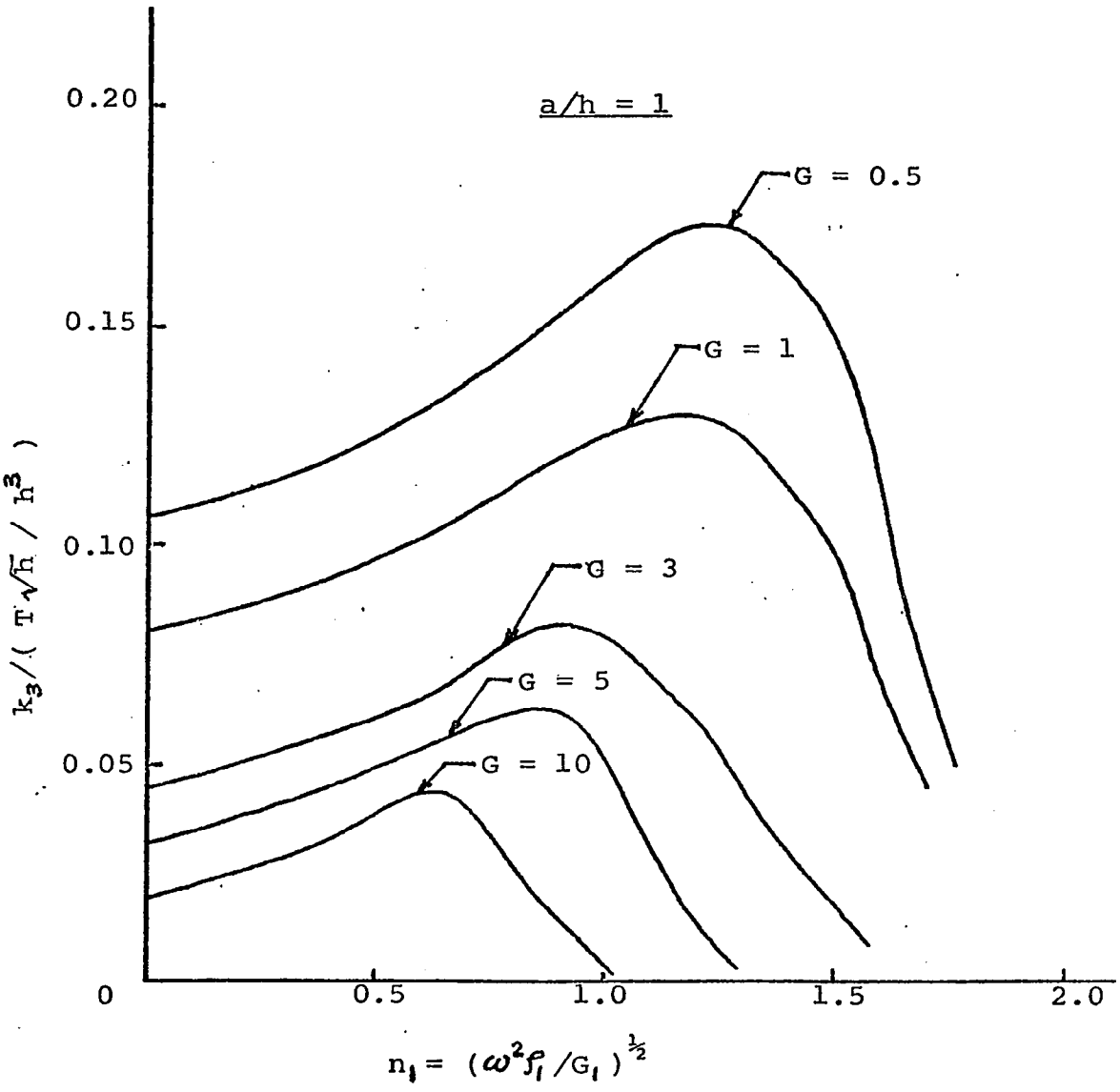

Figure 4. Variation of k_3 with ω for various G-ratios -- Steady State

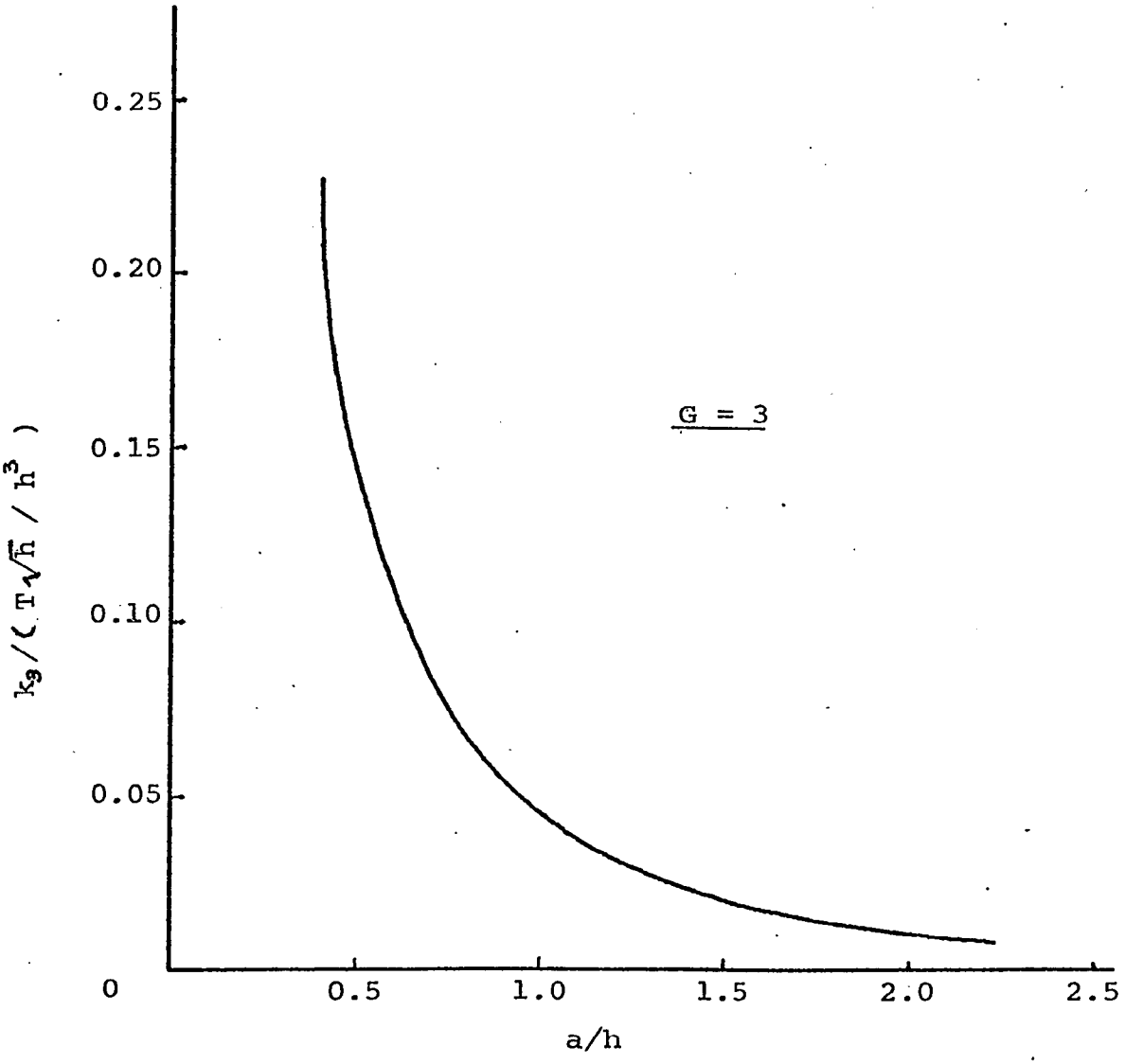

Figure 5. Variation of k_3 with a/h -- Static case: $\omega = 0$

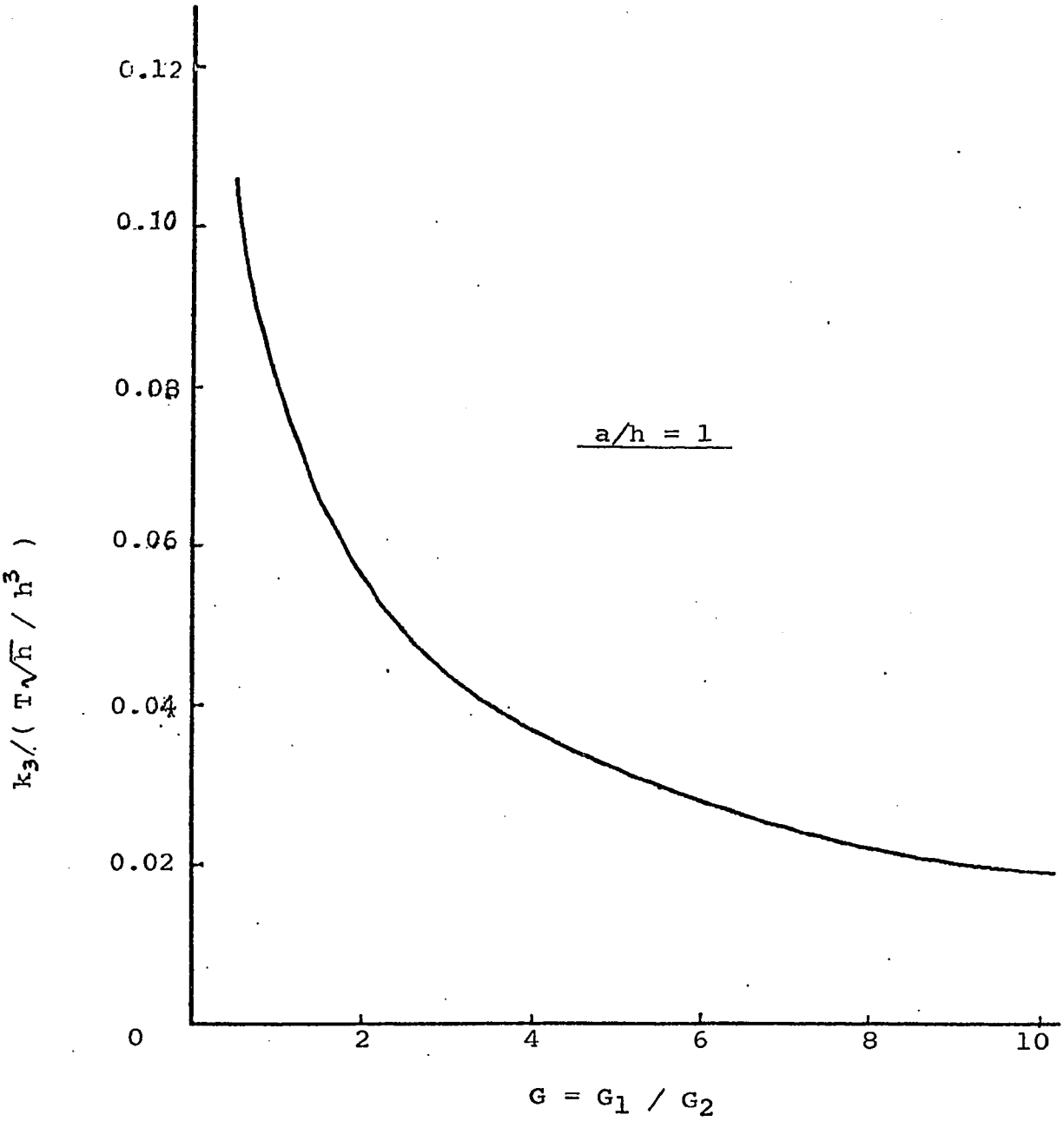

Figure 6. Variation of k_3 with G -- Static case: $\omega = 0$

As expected, the local stress intensification decreases with the increase of crack radius rapidly for lower values of a/h (roughly $a/h \lesssim 1$) and asymptotically for higher values. G vs. k_3 curve experiences monotonic reduction with the increase of G-values, but at a slower rate.

Transient Vibration

The numerical work for the transient vibration is similar to that described for the steady-state condition except that the former is to be performed in the transformed plane, while the latter, of course, is performed in the physical plane. The solution of the Fredholm equation is obtained in the Laplace transform domain and, thus, the determination of $\phi(h,t)$ in equations (3.21) necessitates a numerical inversion of $\bar{\phi}(h,t)/p$. Since this inversion is the only additional numerical work and similar inversions have been covered in many recent publications [28, 29, 30], a general approach of the required numerical treatment is presented in this section along with some numerical results.

In order to express the Fredholm equation in terms of dimensionless parameters, the following notations are introduced in example 1, discussed on page 51

$$t = h\xi$$

$$\theta = h\eta$$

$$s = \lambda/h$$

$$a = \bar{a}h$$

$$\alpha_i \equiv \left(s^2 + \frac{p^2}{c_i^2}\right)^{\frac{1}{2}} = \left(\frac{\lambda^2}{h^2} + \frac{p^2\rho_i}{G_i}\right)^{\frac{1}{2}} = \frac{\gamma_i}{h}$$

$$p = \frac{c_1}{h}(\lambda^2 - \gamma_1^2)^{\frac{1}{2}} = \frac{c_1\bar{p}}{h}$$

$$\bar{\phi}(t,p) = \frac{T_\cdot(1+G)\sqrt{h}}{2\pi^2 h^3 G_1}\,\bar{\Phi}(\xi,\bar{p}) \quad .$$

Making use of these parameters, equations (3.20) assume the

nondimensional form

$$\bar{\Phi}(\xi,\bar{p}) + \int_0^1 \bar{\Phi}(\xi,\bar{p})\bar{L}(\eta,\xi,\bar{p})d\eta = \xi^{\frac{1}{2}}\,\bar{M}(\xi,p) \tag{6.10a}$$

where the symmetrical kernel is

$$\bar{L}(\eta,\xi,\bar{p}) = (\xi\eta)^{\frac{1}{2}} \int_0^\infty \lambda\left[(1+G)\frac{\gamma_1 I_2(\bar{a}\gamma_1)}{\lambda H(\lambda,\bar{p})} - 1\right]\cdot$$

$$\cdot J_0(\lambda\xi)J_0(\lambda\eta)d\lambda \tag{6.10b}$$

and

$$\bar{M}(\xi,\bar{p}) = -\int_0^\infty \gamma_1^2 \left[K_2(\bar{a}\gamma_1) + \left(1 - G\frac{\gamma_1 K_2(a\gamma_1)}{\gamma_2 K_2(a\gamma_2)}\right) I_2(\bar{a}\gamma_1)\frac{K_1(\bar{a}\gamma_1)}{H(\lambda,\bar{p})}\right]\cdot$$

$$\cdot J_0(\lambda\xi)d\lambda \tag{6.10c}$$

The stress-intensity factor from equation (3.21) can now be expressed in terms of the nondimensional auxiliary function $\Phi(\xi,\bar{p})$ as

$$k_3(\bar{T}) = -\frac{T\sqrt{h}}{2\pi^2 h^3}\,\psi(1,\bar{T}) \tag{6.11a}$$

in which

$$\psi(1,\bar{T}) = \frac{1}{2\pi i}\int_{Br} \bar{\psi}(1,\bar{p})\, e^{\bar{p}\bar{T}}\, d\bar{p} \tag{6.11b}$$

and

$$\bar{\psi}(1,\bar{p}) = \frac{\bar{\Phi}(1,\bar{p})}{\bar{p}} \tag{6.11c}$$

In above equations the following dimensionless time variable has been used

$$\bar{T} = \frac{c_1 t}{h}$$

Consider the Laplace transform of $\psi(T)$ defined by the integral

$$\bar{\psi}(p) = \int_0^\infty \psi(\bar{T})\, e^{-p\bar{T}}\, d\bar{T} \qquad (6.12)$$

Since the following discussion will be focused on the transform and its inversion, for convenience, functions $\psi(1,T)$ and $\bar{\psi}(1,\bar{p})$ are abbreviated as $\psi(\bar{T})$ and $\bar{\psi}(\bar{p})$, respectively. The infinite integral in equation (5.10) can be transformed to a finite integral on the interval (-1,1). It follows that $\bar{\psi}(\bar{p})$ can be evaluated from equations (3.20) using an identical procedure as illustrated for the steady-state condition, at the points

$$\bar{p} = (q+1+m)y, \quad m = 0,1,2,...$$

In the above relation, q and y (>0) are real constants and are chosen by judgment based on past experience and trial and error to yield realistic results. For this problem, $q < 2$ and $0.05 \lesssim y \lesssim 2$ can be considered good approximation.

Now, if the substitution

$$x = 2\, e^{-y\bar{T}} - 1 \qquad (6.13)$$

is made in equation (6.10), the following result is obtained

$$\bar{\psi}[(q+1+m) = \frac{1}{2y} \int_{-1}^{1} (1 + \frac{x}{2})^{(q+m)}\, \psi(x)\, dx \qquad (6.14)$$

Then, $\psi(x)$ is expanded into an infinite series of Jacobi polynomials orthogonal on the interval (-1.1). The resultant expression for $\psi(\bar{T})$ that can be used for numerical inversion is

$$\psi(\bar{T}) = \sum_{n=0}^{\infty} C_n P_n^{(o,q)} \quad [2e^{-y\bar{T}} - 1] \tag{6.15a}$$

where C_n can be calculated by the use of orthogonality conditions as follows

$$y\bar{\psi}[(q+1)y] = \frac{C_o}{q+1} \tag{6.15b}$$

$$y\bar{\psi}[(q+2)y] = \frac{C_o}{q+2} + \frac{C_1}{(q+2)(q+3)} \tag{6.15c}$$

$$y\bar{\psi}[(q+3)y] = \frac{C_o}{q+3} + \frac{2C_1}{(q+3)(q+4)} + \frac{2C_2}{(q+3)(q+4)(q+5)} \tag{6.15d}$$

$$y\bar{\psi}[(q+4)y] = \frac{C_o}{q+4} + \frac{3\times1\ C_1}{(q+4)(q+5)} + \frac{3\times2\ C_2}{(q+4)(q+5)(q+6)} + \frac{3!\ C_3}{(q+4)\ldots(q+7)} \tag{6.15e}$$

and so on. Once C_o is determined from the first relation, all other coefficients can be determined in succession from the knowledge of function $\bar{\psi}(\bar{p})$.

For approximate numerical results, the series in equations (6.15) can be truncated at an appropriate point.

Unlike the numerical work for the steady-state condition, the Fredholm equation for the transient vibration is solved

using real arithmetic since γ_i^2 is positive in this case for all values of λ^2. By employing otherwise identical procedure, the auxiliary function $\bar{\phi}(\xi,\bar{p})$ is numerically computed in the transformed plane for various values of $\bar{p}$. Subsequently, by writing a separate program based upon the Laplace transform inversion scheme described above, numerical values of the auxiliary function $\psi(1,\bar{T})$ are obtained where $\bar{\psi}$ and $\bar{\Phi}$ are related by equation (6.11c). Finally, the tearing mode stress-intensity factor is determined from equation (6.11a).

The example of a suddenly applied torque concentrated over a point in the inner cylinder is chosen as an example to illustrate the results. In Fig. 7 and 8, the nondimensional stress-intensity factor is plotted against the dimensionless time variable $\bar{T}$ for modular ratio $G_1/G_2 = 3$ and crack dimension $a/h = 1$. The transient effect is observed as k_3 first reaching a peak and then oscillating about the static value with decreasing amplitude. The peak is observed to be about 40% higher than the static value and to occur at about $\bar{T} = 2.5$ for the particular crack geometry and material properties. As time $\bar{T}(= \frac{c_1 t}{h})$ increases, the value of k_3 approaches that of the static case.

In summary, one observes that the elastodynamic stress-intensity factor k_3 can be expressed as

$$k_3(t) = F(t)\,(k_3)_{static}$$

where $F(t)$ is some function representing the difference

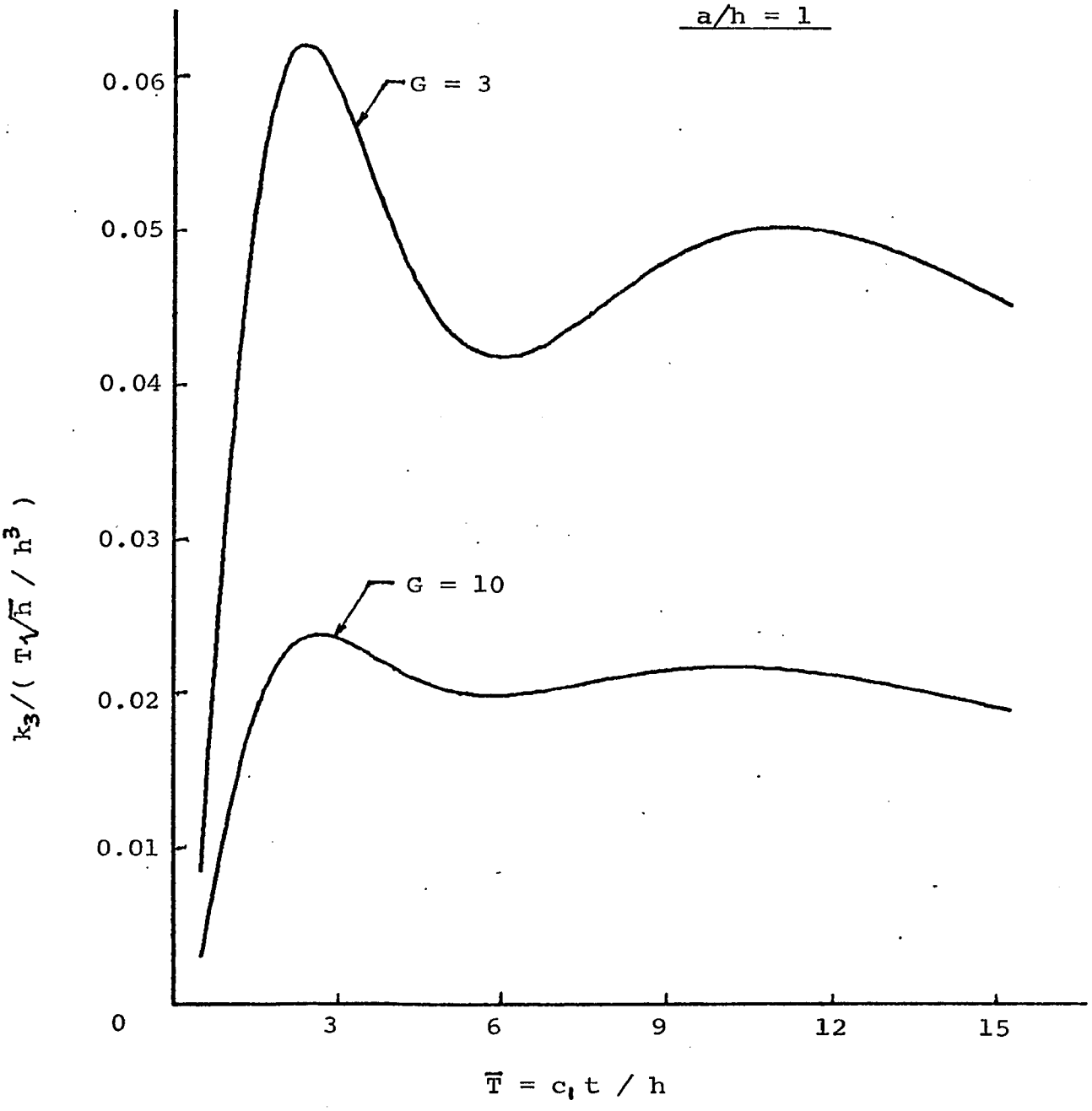

Figure 7. variation of k_3 with time -- Transient

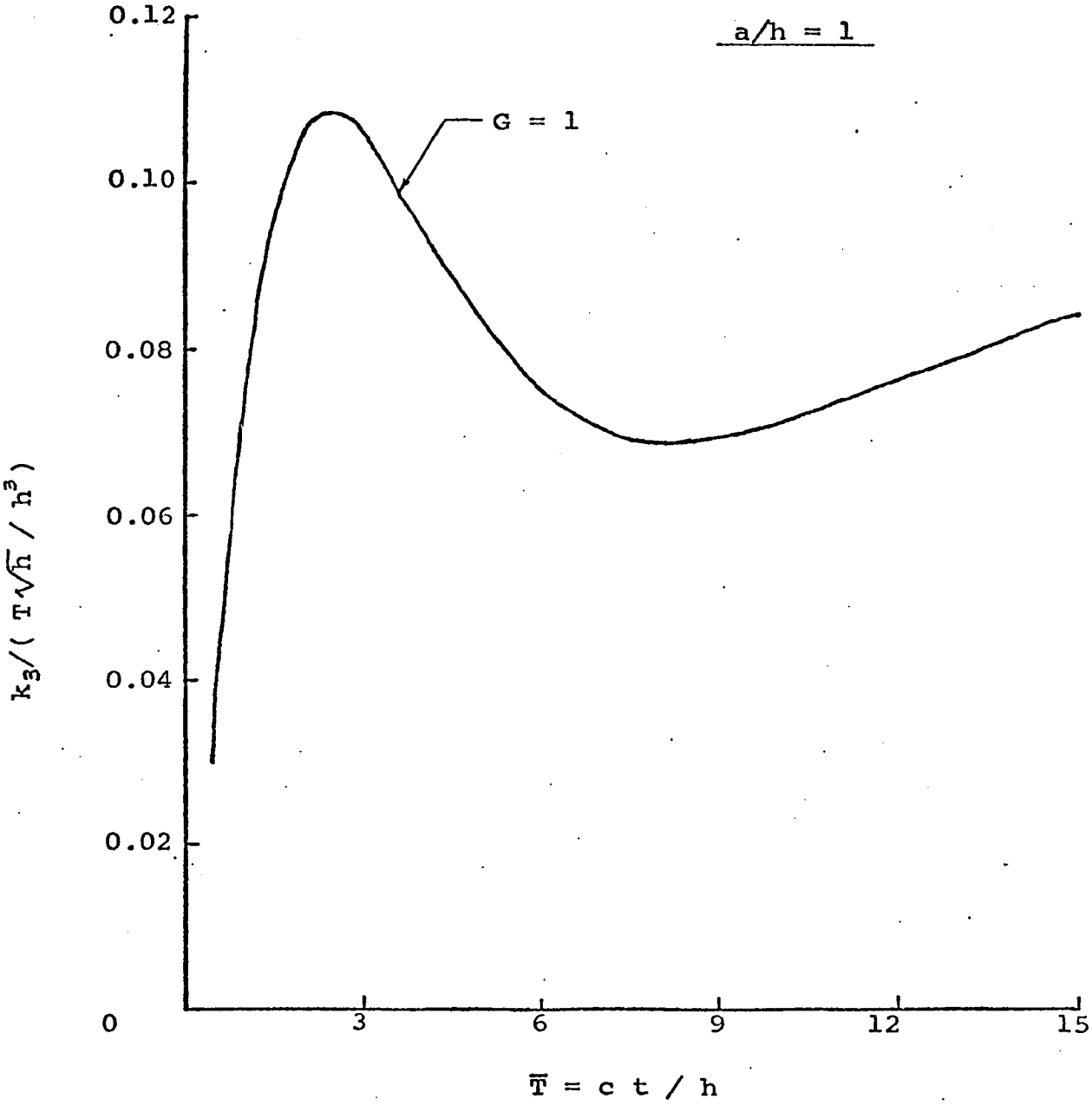

Figure 8. Variation of k_3 with time for a homogeneous medium -- Transient

between the static value of k_3 and the dynamic one. For impulsive torsional loading on the exposed end of the composite, it is found that F(t) increases monotonically to a number close 1.40 and then oscillates with decreasing amplitudes about unity. The dynamic overshoot in this case is about 40%. This behavior is in agreement with the results for "sudden twisting of a penny-shaped crack" [22].

Chapter 7

CONCLUSION

In this concluding chapter, the results obtained in previous chapters will be summarized, the practical application of this research work will be discussed, and possible future research works employing the techniques and results presented in this dissertation will be hinted upon.

Summary of Results

Analogous to any dynamic problem, the cracked cylinders treated in the dissertation under the application of torsional vibration, are observed to experience dynamic amplification of local stress fields. This amplification is excited as an interaction between the impounding forcing function and the inherent physical characteristics of the media. The maximum intensification can be compared to the resonance of other vibration problems.

The steady-state vibration can amplify the static stress-intensity factor by as much as two at a certain frequency level of the input motion depending upon physical properties and crack geometrics. Such vibration is characterized by producing a peak and then having almost no effect at high frequencies.

On the other hand, the Heaviside transient forcing function results in numerous peaks, the first one being prominent

with about 40% to 50% amplification over the static value. Unlike the steady-state vibration, the dynamic stress-intensity factor for the transient case oscillates about the static value and approaches that with time.

Practical application of the results obtained in the dissertation can be found in fracture mechanics, where two media are bonded together, having a finite flaw at one side of the common boundary. Other practically oriented problems can be solved as corollaries using the techniques presented in this research work.

Suggestion for Future Research

The solution obtained in Chapter 2 for steady-state vibration of a half-space, can be improved to ensure the assumption that only outward waves prevail. This can probably be accomplished by manipulating the input wave function in in equations (2.5) and (2.6).

In this dissertation, the load transfer problem between two partially bonded cylinders subjected to torsional vibration is studied. The external loading is imparted to the composite by specifying known shear stresses over the contact surface within the inner cylinder. A further involved situation will arise if the displacement is specified over the entire inner cylinder $0 \leq r \leq a$ (Fig. 1). This can be physically achieved by twisting a disk rigidly attached to the inner cylinder by a constant angle, γ. The boundary conditions at the contact surface ($z = 0$) will then be as follows:

$$u_\theta = \gamma r, \qquad 0 \leq r \leq a$$
$$\tau_{\theta z} = 0 \qquad\qquad r > a$$

The remaining boundary conditions are the same as in the dissertation. This problem can be considered as a special application of the well-known Reissner-Sagoci problem [31], and can be solved adopting a procedure similar to that employed in this dissertation. Based upon previous research works performed on this type of Reissner-Sagoci problem, it seems that there may exist a stress singularity other than the square root singularity at the crack tip [32,33]. The static solution of this problem can be found in the works of Prasad and Chatterjee [33].

Following the approach presented in this dissertation, several other related problems can be solved. One such problem is the study of the same crack geometry of Fig. 1 with a finite-radius outer cylinder under the application of a dynamic radial pull on the external cylindrical surface. Under this normal loading, the stress-intensity factor, k_1, for the opening mode can be obtained. Assuming b is the outer radius, the boundary condition on the external surface, i.e. for r = b, is

$$\sigma_r = p(z,t) \qquad h_1 \leq z \leq 0$$
$$= 0 \qquad\qquad z > h_1$$

where h_1 is the height of the cylinder subjected to the known external pressure p.

APPENDICES

APPENDIX A

Solution of the Displacement Equilibrium Equation (2.7)

The solution of the equilibrium equation (2.8) will be sought by use of classical separation of variable technique [25]. The displacement u_θ^* which is a function of r and z, can be assumed as a product of two new functions, one a function of r and the other a function of z only, i.e.

$$u_\theta^*(r,z) = R(r) \cdot Z(z)$$

Inserting this new definition of u_θ in equation (2.7), the differential equation yields

$$\frac{R''}{R} + \frac{1}{r}\frac{R'}{R} - \frac{1}{r^2} = -\frac{z''}{z} - n_i^2 = \text{constant} = \pm s^2, \text{ say}$$

In the above equation, a single prime denotes differentiation once and a double prime denotes differentiation twice, both with respect to the corresponding variable. For two different constants, two different solutions will be obtained, and when combined will provide a complete solution.

Case 1: constant $= -s^2$

Therefore, $z'' - (s^2 - n_i^2)z = 0$

which is satisfied by $z \sim e^{-z(s^2-n_i^2)^{\frac{1}{2}}}$

and $r^2R'' + rR' + (s^2r^2 - 1)R = 0$

which is satisfied by $R \sim J_1(rs)$

Therefore, the solution is

$$u_\theta^*(r,z) = \int_o^\infty A(s)\ J_1(rs)e^{-z(s^2-n_i^2)^{\frac{1}{2}}}ds \qquad (A1)$$

as indicated in equation (2.8a)

Case 2:

Costant = s^2

Therefore, $z'' + (s^2+n_i^2)z = 0$

which yields $z \sim \cos[(s^2+n_i^2)^{\frac{1}{2}}z]$

and $r^2R'' + rR' - (s^2r^2+1)R = 0$

which yields $R \sim I_1(rs)$ or $K_1(rs)$

Therefore, the solution is

$$u_\theta^*(r,z) = \int_o^\infty B(s) \begin{bmatrix} I_1(r\sqrt{s^2-n_i^2}) \\ K_1(r\sqrt{s^2-n_i^2}) \end{bmatrix} \cos(sz)ds \qquad (A2)$$

Whether the solution will involve the modified Bessel function I_1 or K_1, depends on the boundary conditions, and that one will be chosen which assures finite displacement everywhere in the region. Since s is a dummy variable, $(s^2+n_i^2)$ has been replaced by s^2 in the above derivation. The resulting expressions for the displacement are given in equations (2.9) and (2.10).

APPENDIX B

Solution of the Dual Integral Equations (2.31)

The solution of the dual integral equations (2.31) will be obtained following Snedden's approach [24].

Inserting the definition of N(s) from equation (2.32) in equation (2.31b) and interchanging the order of integration, one obtains

$$\int_o^h \phi^*(t)\left[\int_o^\infty J_o(st)\cos(sz)\,ds\right]dt = 0, \quad z > h \tag{B1}$$

Noting that $t \leq h < z$, and using the identity [23]

$$\int_o^\infty J_o(st)\cos(sz)\,ds = 0, \quad t < z \tag{B2}$$

it can be easily proved that equation (2.31b) is automatically satisfied by the definition of N(s) chosen in equation (2.32).

To obtain a solution of $\phi^*(t)$, rewrite equation (2.31a) as

$$\frac{d}{dz}\left[\int_o^\infty N(s)\,\sin)(sz)\,ds\right] = (1+G)W(z) + \int_o^\infty s[1-F(\alpha_1)]N(s)\cos(sz)ds, \quad 0 \leq z \leq h \tag{B3}$$

Replace N(s) in the left hand side of the above equation, by equation (2.32), so that equation (B3) takes the form

$$\frac{d}{dz}\int_o^z \frac{\phi^*(t)dt}{(z^2-t^2)^{\frac{1}{2}}} = (1+G)W(z) + \int_o^\infty s\,[1+F(\alpha_1)]N(s)\cdot$$

$$\cdot\cos(sz)ds \qquad \text{(B4)}$$

This is a standard Abbel integral equation with the solution [24]

$$\phi^*(t) = \frac{2}{\pi}(1+G)t\int_o^t \frac{W(z)dz}{(t^2-z^2)^{\frac{1}{2}}} + \frac{2}{\pi}t\int_o^t \frac{1}{(t^2+z^2)^{\frac{1}{2}}}\cdot \qquad \text{(B5)}$$

$$\cdot\left[\int_o^\infty s[1-F(\alpha_1)]N(s)\cos(sz)\cdot ds\right]dz$$

Noting that $\int_o^t \frac{\cos(sz)}{(t^2-z^2)^{\frac{1}{2}}}dz = \frac{\pi}{2}J_o(st)$,

one gets

$$\phi^*(t) = \frac{2}{\pi}(1+G)t\int_o^t \frac{W(z)dz}{(t^2-z^2)^{\frac{1}{2}}} + t\int_o^\infty s\,[1-F(\alpha_1)]N(s)\cdot$$

$$\cdot J_o(st)ds \qquad \text{(B6)}$$

Rearranging terms, $\phi^*(t)$ is given by

$$\phi^*(t) + t\int_o^\infty s\,[F(\alpha_1)-1]\,J_o(st)\left[\int_o^h \phi(\theta)J_o(s\theta)d\theta\right]ds$$

$$= \frac{2}{\pi}(1+G)\,t\int_o^t \frac{W(z)dz}{(t^2-z^2)^{\frac{1}{2}}} \qquad \text{(B7)}$$

This can be further simplified to result in a standard Fredholm equation of the second kind

$$\phi^*(t) + \int_o^h \phi^*(\theta)K(\theta,t)d\theta = \frac{2}{\pi}(1+G)t\int_o^t \frac{W(z)dz}{(t^2-z^2)^{\frac{1}{2}}} \qquad \text{(B8a)}$$

where the kernel stands for

$$K(\theta,t) = t \int_0^\infty s[F(\alpha_1) - 1]J_0(st)J_0(s\theta)ds \qquad \text{(B8b)}$$

which are stated in equations (2.33).

APPENDIX C

Evaluation of Integrals in Equations (2.31d) and (2.33a)

The right-hand side integral in equation (2.33a) is free from the auxiliary function $\phi^*(t)$, and can be evaluated in terms of the prescribed stress function $\tau_o(r)$. To this end, make use of equation (2.31d) to obtain the following solution by rearranging terms

$$\int_o^t \frac{W(z)}{(t^2-z^2)^{\frac{1}{2}}}\,dz = \int_o^t \frac{f(z)\,dz}{(t^2-z^2)^{\frac{1}{2}}} - \frac{2}{\pi}\int_o^\infty \alpha_1 \left(\frac{1}{G_1} - \frac{\alpha_1 K_2(a\alpha_1)}{G_2\alpha_2 K_2(a\alpha_2)}\right) \cdot$$

$$\cdot I_2(a\alpha_1)\,\frac{K_1(a\alpha_2)}{H(s)}\left[\int_o^t \frac{\cos(s\,z)\,dz}{(t^2-z^2)^{\frac{1}{2}}}\right.$$

$$\left.\cdot\int_o^b r\,I_1(r\alpha_2)\,\tau_o(r)\,dr\right]\,ds \qquad \text{(C1)}$$

With the help of the identity

$$\int_o^t \frac{\cos(sz)\,dz}{(t^2-z^2)^{\frac{1}{2}}} = J_o(st) \qquad \text{(C2)}$$

the above equation reduces to

$$\int_o^t \frac{W(z)dz}{(t^2-z^2)^{\frac{1}{2}}} = \int_o^t \frac{f(z)\ dz}{(t^2-z^2)^{\frac{1}{2}}} - \int_o^\infty \alpha_1 \left\{ \frac{1}{G_1} - \frac{\alpha_1 K_2(a\alpha_1)}{G_2 \alpha_2 K_2(a\alpha_2)} \right\} J_o(st)$$

$$\cdot I_2(a\alpha_1)\ \frac{K_1(a\alpha_2)}{H(s)} \left[\int_o^b r I_1(r\alpha_1)\tau_o(r)dr \right] ds \qquad \text{(C3)}$$

In order to evaluate $\int_o^t \frac{f(z)\ dz}{(t^2-z^2)^{\frac{1}{2}}}$, insert equation (2.22) in equation (2.18b) and invert by the Fourier cosine transform to yield

$$f(z) = -\frac{2}{\pi G_1} \int_o^\infty \cos(sz)\alpha_1 K_2(a\alpha_1) \left[\int_o^b r\tau_o(r) I_1(r\alpha_1)dr \right] ds \qquad \text{(C4)}$$

Hence,

$$\int_o^t \frac{f(z)}{(t^2-z^2)^{\frac{1}{2}}} dz = -\frac{2}{\pi G_1} \int_o^t \frac{1}{(t^2-z^2)^{\frac{1}{2}}} \left[\int_o^\infty \cos(sz)\alpha_1 K_2(a\alpha_1) \cdot \left\{ \int_o^b r\tau_o(r) I_1(r\alpha_1)dr \right\} \right] ds \qquad \text{(C5)}$$

Rearranging the order of integration and performing a simple integration, it follows

$$\int_o^t \frac{f(z)}{(t^2-z^2)^{\frac{1}{2}}}\ dz = -\frac{1}{G_1} \int_o^\infty \alpha_1 J_o(st) K_2(as) \cdot \left[\int_o^b r\tau_o(r) I_1(r\alpha_1)d\eta \right] ds \qquad \text{(C6)}$$

Using this result in equation (C3), one finally obtains

$$\int_o^t \frac{W(z)dz}{(t^2-z^2)^{\frac{1}{2}}} = -\int_o^\infty \left[\frac{\alpha_1}{G_1} K_2(a\alpha_1) + \left(\frac{1}{G_1} - \frac{\alpha_1 K_2(a\alpha_1)}{G_2\alpha_2 K_2(a\alpha_2)}\right)\alpha_1 \cdot \right.$$

$$\left. \cdot I_2(a\alpha_1)\ \frac{K_1(a\alpha_2)}{H(s)}\right] J_o(st)$$

$$\cdot\left[\int_o^b r\ I_1(r\alpha_1)\tau_o(r)dr\right] ds \qquad (C7)$$

which is the result given in equation (2.34).

References

1. Griffith, A.A. "The Phenomena of Rupture and Flow in Solids." Philosophical Transactions, Royal Society of London, Series A221, 1921, pp. 163-198.

2. Irwin, G.R. "Crack Extension Force for a Part-through Crack in a Plate." Journal of Applied Mechanics, ASME Transaction Vol. 84, 1962, pp. 651-654.

3. Snedden, I.N. and Lowengrub, M. Crack Problems in the Classical Theory of Elasticity. John Wiley and Sons, Inc., New York, 1969.

4. Kassir, M.K. and Sih, G.C. Three Dimensional Crack Problems, Mechanics of Fracture 2. Noordhoff International Publishing, The Netherlands, 1975.

5. Williams, M.L. "The Stresses around a Fault or Crack in Dissimilar Media." Bulletin of the Seismological Society of America, 49, 1959, pp. 199-204.

6. Sih, G.C. and Rice, J.R. "The Bending of Plates of Dissimilar Materials with Cracks." Journal of Applied Mechanics, ASME Transaction Vol. 86, 1964, pp. 477-482.

7. Yoffé, E.H. "The Moving Griffith Crack." The Philosophical Magazine, Vol. 42, 1951, pp. 739-750.

8. Craggs, J.W. "On the Propagation of a Crack in an Elastic-Brittle Material." Journal of the Mechanics and Physics of Solids, Vol. 8, 1960, pp. 66-75.

9. Bilby, B.A. and Bullough, R. "The Formation of Twins by a Moving Crack." The Philosophical Magazine, Vol. 45, 1954, pp. 631-646.

10. McClintock, F.A. and Sukhatme, S.P., "Travelling Cracks in Elastic Materials under Longitudinal Shear." Journal of the Mechanics and Physics of Solids, Vol. 8, 1960, pp. 187-193.

11. Broberg, B. Arkiv. Fysik, Vol. 18, 1960, p. 159.

12. Barenblatt, G.I., Salganik, R.L. and Cherepanov, G.P. "On the Nonsteady Propagation of Cracks." Journal of Applied Mathematics and Mechanics (PMM), Vol. 26, pp. 469-477.

13. Craggs, J.W. Fracture of Solids. John Wiley and Sons, New York, 1963.

14. Kostrov, B.V. "The Axisymmetric Problem of Propagation of a Tension Crack." Journal of Applied Mathematics and Mechanics (PMM), Vol. 28, 1964, pp. 793-803.

15. Loeber, G.F. and Sih, G.C. "Torsional Vibration of an Elastic Solid Containing a Penny-shaped Crack." The Journal of the Acoustical Society of America, Vol. 44, 1968, pp. 1237-1245.

16. Maue, A.W. "Die Entspannungswelle bei plötzlichem Einschnitt eines gespannten elastischen Körpers." Zeitschrift für Angewandte Mathematik und Mechanik, Vol. 34 1954, pp. 1-12.

17. Ang, D.D. "Some Radiation Problems in Elastodynamics." Dissertation, California Institute of Technology, Pasadena, California, 1958.

18. Baker, B.R. "Dynamic Stresses Created by a Moving Crack." Journal of Applied Mechanics, ASME Transaction Vol. 84, Series E, 1962, pp. 449-458.

19. Ravera, R.J. and Sih, G.C. "Transient Analysis of Stress Waves Around Cracks Under Antiplane Strain." Journal of the Acoustical Society of America, Vol. 47, 1970, pp. 875-881.

20. Sih, G.C. and Loeber, J.F. "Normal Compression and Radial Shear Waves Scattering at a Penny-shaped Crack in an Elastic Solid." Journal of the Acoustical Society of America, 46, 1969, pp. 711-721.

21. Robertson, I.N. "Diffraction of a Plane Longitudinal Wave by a Penny-shaped Crack." Proceedings of Cambridge Philosophical Society, 63, 1967, pp. 229-238.

22. Sih, G.C. and Embley, G.T. "Sudden Twisting of a Penny-shaped Crack to Impact Waves." Proceedings of the 12th Midwestern Mechanics Conference, 6, 1972, pp. 473-487.

23. Erdelyi, A., Editor. Tables of Integral Transforms, 2. McGraw-Hill, Inc., New York, 1954.

24. Snedden, I.N. Mixed Boundary Value Problems in Pontential Theory. North-Holland Publishing Co., Amsterdam, The Netherlands, 1966.

25. Hildebrand, F.B. Advanced Calculus for Applications. Prentice-Hall, New Jersey, 1962.

26. Sih, G.C. "Dynamic Aspects of Crack Propagation." Inelastic Behavior of Solids. Ed. M.F. Kanninen et al. McGraw-Hill, New York, 1969, pp. 607-639.

27. Kantorvich, L.V. and Krylov, V.I. Approximate Methods of Higher Analysis. Interscience Publishers, New York, 1958.

28. Papoulis, A. "A New Method of Inversion of the Laplace Transform." Quarterly of Applied Mathematics, Vol. 14, 1957, pp. 405-414.

29. Weeks, W.T. "Numerical Inversion of Laplace Transforms Using Laguerre Functions." Journal of the Association of Computing Machinery, Vol. 13, No. 3, 1966, pp. 419-426.

30. Miller, M.K. and Guy, W.T. "Numerical Inversion of the Laplace Transform by Use of Jacobi Polynomials." SIAM, Journal of Numerical Analysis, 3, 1966, pp. 624-635.

31. Reissner, E. and Sagoci, H.F. "Forced Torsional Oscillations of an Elastic Half Space-I." Journal of Applied Physics, Vol. 15, 1944, p. 652.

32. Freeman, N.J. and Keer, L.M. "Load Transfer Problem for an Embedded Shaft in Torsion." Journal of Applied Mechanics, ASME Transaction, Vol. 92, 1970, pp. 959-964.

33. Prasad, S.N. and Chatterjee, S.N. "Load Transfer in Torsion of Compound Cylinders with a Cylindrical Crack." Journal of Applied Mechanics, Transaction of the ASME, September 1973, pp. 773-779.

34. Noble, B. Methods Based on the Weiner-Hopf Technique. Pergamon Press, Inc., New York, 1958.

VITA

Kamal Bandyopadhyay pursued his undergraduate study in civil engineering in Bengal Engineering College of the University of Calcutta, India. He graduated with a Bachelor of Engineering degree in 1967.

From 1967 to 1971, Mr. Bandyopadyay worked in various aspects of civil engineering in construction and design. In 1971, he immigrated to the United States and continued rendering professional services to Amman and Whitney Associates and other engineering firms. In 1973, Mr. Bandyopadhyay began his graduate studies at The City College of New York. He received the Master of Engineering degree in 1975, and continued the doctoral program in The City University of New York.

A Professional Engineer registered in New York State, Mr. Bandyopadhyay is currently employed by Gibbs & Hill, New York, in the position of a Senior Engineer in their Special Analysis group.

Mr. Bandyopadhyay co-authored a paper on "Contact Problems for Solids Containing Cavities," published in the Journal of the Engineering Mechanics Division, ASCE, Vol. 104, in December, 1978.